

Injection mechanisms of short-lived radionuclides and their homogenization

N. Ouellette^{a,*}, S.J. Desch^b, M. Bizzarro^c, A.P. Boss^d, F. Ciesla^d, B. Meyer^e

^a *Laboratoire d'Étude de la Matière Extraterrestre, Museum National d'Histoire Naturelle USM 0205, CP 52, 61 rue Buffon, 75005 Paris, France*

^b *School of Earth and Space Exploration, Arizona State University, P.O. Box 871404, Tempe, AZ 85287-1404, USA*

^c *Geological Institute, University of Copenhagen, Øster Voldgade 10, DK-1210 København K, Denmark*

^d *Department of Terrestrial Magnetism, Carnegie Institution of Washington, 5241 Broad Branch Road, N.W., Washington, DC 20015, USA*

^e *Department of Physics & Astronomy, Clemson University, 118 Kinard Laboratory, Clemson, SC 29634-0978, USA*

Received 3 March 2008; accepted in revised form 15 October 2008; available online 20 May 2009

Abstract

The supernova injection model for the origin of the short-lived radionuclides (SLRs) in the early solar system is reviewed. First, the meteoritic evidence supporting the model is discussed. Based on the presence of ⁶⁰Fe it is argued that a supernova must have been in close proximity to the nascent Solar System. Then, two models of supernova injection, the supernova trigger model and the aerogel model, are described in detail. Both these injection model provide a mechanism for incorporating SLRs into the early solar system. Following this, the mechanisms present in the disk to homogenize the freshly injected radionuclides, and the timescales associated with these mechanisms, are described. It is shown that the SLRs can be homogenized on very short timescales, from a thousand years up to ~1 million years. Finally, the SLR ratios expected from a supernova injection are compared to the ratios measured in meteorites. A single supernova can inject enough radionuclides to explain the radionuclide abundances present in the early solar system.

© 2009 Elsevier Ltd. All rights reserved.

1. INTRODUCTION

The discovery that meteorites and their components contain traces of (now extinct) short-lived radionuclides (SLRs) has revolutionized the field of meteoritics and our understanding of the formation of our Solar System. At this juncture, nine SLRs with half-lives of 16 Myr or less have been confirmed to have existed in the early Solar System. The existence and inferred abundances of these SLRs place exacting constraints on their origins: the high abundance of ⁶⁰Fe in the early Solar System argues strongly for injection of this isotope from an external, stellar nucleosynthetic source. Conversely, the existence of ¹⁰Be argues for a separate origin involving spallation reactions and high-energy particles in some location, perhaps near the early Sun. Many SLRs are also used as chronometers: Al–Mg systematics that probe

the decay of ²⁶Al, and Mn–Cr systematics that probe the decay of ⁵³Mn, reveal time differences between formation (isotopic closure) of various meteoritic components on ~1 Myr timescales. The use of these isotopes as chronometers is, however, predicated on two assumptions: (1) that the SLRs ²⁶Al and ⁵³Mn were distributed homogeneously throughout the Solar System at an early time and (2) the abundances of these isotopes changed only because of radioactive decay, and were not increased by continued contributions over Solar System history. In other words, the use of SLRs as chronometers is complicated if they are produced within the Solar System, but SLRs can readily and validly be used as chronometers if they are injected into the Solar System from an external source, and then quickly mixed. The purpose of this paper is to review the evidence for injection and rapid mixing of SLRs.

This paper is organized into five sections. In Section 2 we review the meteoritic evidence for the one-time presence

* Corresponding author. Fax: +33 480 965 7654.
E-mail address: nouvellet@mnhn.fr (N. Ouellette).

of SLRs in the early Solar System, especially the evidence for injection and homogenization of these isotopes. In Section 3 we discuss two models for the injection of SLRs from a nearby supernova, the “supernova trigger” model in which a supernova triggers the collapse of a cloud core and injects radionuclides into it, and the “aerogel” model in which a supernova injects SLRs into an extant protoplanetary disk. We discuss the subsequent mixing of isotopes in the context of these models in Section 4. In Section 5 we offer predictions for the abundances of SLRs and compare them to the meteoritic record. We conclude in Section 6 that injection of SLRs by a nearby supernova, and mixing within the disk, are completely consistent with the predictions of theoretical models and with the meteoritic record.

2. METEORITIC EVIDENCE

Short-lived radionuclides have provided critical insights into the formation and evolution of the early Solar System in the four decades since they were first discovered. Following the detection of excess ^{129}Xe related to the *in situ* decay of ^{129}I in primitive meteorites by Reynolds (1960) – the first evidence for the former presence of a SLR in the early Solar System – approximately one dozen SLRs with half-lives ($T_{1/2}$) ranging from ~ 0.1 to >100 Myr are now inferred to have existed at the time most meteorites formed (Table 1). Whereas early Solar System abundances of short-lived isotopes with relatively long half-lives like ^{53}Mn and ^{182}Hf might broadly reflect input from stellar sources over the history of our Galaxy, the inferred levels of ^{41}Ca , ^{26}Al , ^{60}Fe and ^{10}Be are too high to uniquely derive from Galactic production (Jacobsen, 2005; Huss et al., 2008). Their abundances require that these nuclides were synthesized in a stellar environment and injected into the protosolar molecular cloud at the time of its collapse or, alternatively, into the active protoplanetary disk (Ouellette et al., 2007a,b). The competing X-wind model proposes that SLRs are the product of interactions of solar energetic particles with gas and dust in the protoplanetary disk (Shu et al., 1996, 1997, 2001; Lee et al., 1998; Gounelle et al.,

2001; Gounelle, 2006). The reader is referred to these papers and Wadhwa et al. (2007) for a complete description of this model. In this section, we briefly review the state-of-the-knowledge regarding the initial abundances and distribution of key SLRs that impact the understanding of their origin and injection mechanism(s) into the nascent Solar System.

2.1. The initial abundances and distribution of ^{10}Be , ^{26}Al , ^{41}Ca and ^{60}Fe

2.1.1. ^{10}Be – ^{10}B ($T_{1/2} \sim 1.5$ Myr)

Beryllium-10 is unique amongst SLRs in that it is destroyed by stellar nucleosynthesis and is formed by spallation reactions when energetic ($> \text{MeV/nucleon}$) ions collide with and spall heavier nuclei, usually O. Beryllium-10 thus provides unique information on irradiation processes that affected early solar system processes. Excess ^{10}B clearly linked to the *in situ* decay of ^{10}Be was first detected in a calcium-aluminum-rich inclusion (CAI) from the Allende meteorite by McKeegan et al. (2000). Following this discovery, a number of studies have demonstrated the widespread distribution of ^{10}Be in CAIs from various chondrites (Marhas et al., 2002; MacPherson et al., 2003; Chaussidon et al., 2006), with inferred initial $^{10}\text{Be}/^9\text{Be}$ ratios at the time of CAI formation ranging from $(0.4 \pm 0.1) \times 10^{-3}$ to $(1.8 \pm 0.5) \times 10^{-3}$. Liu et al. (2007) report an initial value of $^{10}\text{Be}/^9\text{Be} = (5.1 \pm 1.4) \times 10^{-4}$ in a hibonite that did not initially contain measurable ^{26}Al , and assert that factor of two variations in $^{10}\text{Be}/^9\text{Be}$ rule out Galactic cosmic rays trapping of ^{10}Be (see below). Still, the number of analyses remains relatively small, and further studies are needed to assess the statistical significance of the observed variations in initial abundances of ^{10}Be in CAIs. It remains unclear whether they reflect variable production of this nuclide by irradiation, spatial variation in GCR trapping efficiency, a time difference in the formation history of these objects or, alternatively, a late-stage perturbation. Evidence for the former presence of ^{10}Be has also been found in hibonites from the Murchison meteorite, at levels that are consistent with the initial ^{10}Be abundance inferred from various CAIs. Importantly, the Murchison hibonites show no evidence for the decay of ^{41}Ca or ^{26}Al . Severe limits on their initial abundances have been imposed (Marhas et al., 2002) that are not apparently consistent with models of the concurrent production of ^{10}Be , ^{41}Ca and ^{26}Al within Solar System solids, such as expected from the X-wind model (Gounelle et al., 2001). During the collapse of the molecular cloud from which the Solar System formed, low-energy Galactic cosmic rays that are the nuclei of ^{10}Be atoms would have been trapped within it, at levels consistent with the inferred initial abundances of ^{10}Be (Desch et al., 2004). This is consistent with the ubiquitous presence of ^{10}Be even in the Murchison hibonites, and strengthens the case for a later injection of ^{41}Ca and ^{26}Al from a stellar source.

2.1.2. ^{26}Al – ^{26}Mg ($T_{1/2} \sim 0.73$ Myr)

Following the initial discovery for live ^{26}Al in an Allende CAI by Lee et al. (1976), it is now firmly established that

Table 1
Data on short-lived radionuclides.

Radionuclide	Reference isotope	$T_{1/2}$ (Myr)	Initial value
^{41}Ca	^{40}Ca	0.10	1.4×10^{-8}
^{36}Cl	^{35}Cl	0.30	3.0×10^{-6}
^{26}Al	^{27}Al	0.73	$5\text{--}7 \times 10^{-5}$
^{10}Be	^9Be	1.5	1.0×10^{-3}
^{60}Fe	^{56}Fe	1.5	$3\text{--}10 \times 10^{-7}$
^{53}Mn	^{55}Mn	3.7	$1\text{--}2 \times 10^{-5}$
^{107}Pd	^{108}Pd	6.5	5.0×10^{-5}
^{182}Hf	^{180}Hf	9	1.1×10^{-4}
^{205}Pb	^{204}Pb	15	$\sim 1.0 \times 10^{-4}$
^{129}I	^{127}I	16	1.4×10^{-4}
^{92}Nb	^{90}Nb	36	1×10^{-5}
^{146}Sm	^{144}Sm	103	5×10^{-3}

Adapted from Wasserburg et al. (1994), Birk (2004), Wadhwa et al. (2007) and Baker et al. (2007).

^{26}Al was widespread and apparently homogeneously distributed within the inner Solar System. Indeed, evidence for the former presence of ^{26}Al has been documented using *in situ* methods in a range of objects including various types of CAIs, chondrules and differentiated planetesimals, with an inferred Solar System (apparently homogeneous) initial $^{26}\text{Al}/^{27}\text{Al}$ ratio of $\sim 5 \times 10^{-5}$ (MacPherson et al., 1995; Kita et al., 2005; Srinivasan et al., 1999). Taking advantage of improved methods for high-precision measurements of Mg isotopes, recent reports – although not all (Jacobsen et al., 2008) – have called for an upward revision of the initial $^{26}\text{Al}/^{27}\text{Al}$ ratio to $\sim 6 \times 10^{-5}$ (Young et al., 2005; Thrane et al., 2006). Importantly, high-precision measurements of Mg isotopes in bulk CAIs now define an isochron with a negative initial ^{26}Mg abundance ($^{26}\text{Mg}^* = -0.0317 \pm 0.0038\%$) with respect to analyses of samples from Earth, the Moon, Mars and chondrite meteorites (Bizzarro et al., 2004, 2005; Baker et al., 2005; Thrane et al., 2006). This observation unequivocally demonstrates that ^{26}Al was present in the accretion region of terrestrial planets and planetesimals at levels that are broadly comparable to those present in CAIs, thereby supporting the homogeneous distribution of ^{26}Al in the inner Solar System. Homogeneous distribution can be readily achieved if ^{26}Al was produced by stellar nucleosynthesis in a supernova, an asymptotic giant branch star, or a Wolf–Rayet (WR) star, and injected into the Solar System's parental molecular cloud or, alternatively, into the active protoplanetary disk (Boss, 2007); however, it is now clear that some primitive and refractory objects like FUN-type (Fractionation and Unknown Nuclear effects) CAI inclusions contain no evidence for ^{26}Al (upper limits $^{26}\text{Al}/^{27}\text{Al} < 5 \times 10^{-8}$; Fahey et al., 1987), and this is commonly interpreted as reflecting formation prior to the injection and/or homogenization of ^{26}Al in the nascent Solar System (Sahijpal and Goswami, 1998; MacPherson, 2003; Thrane et al., 2008). These observations collectively support a stellar origin for ^{26}Al and, hence, chronological significance of the ^{26}Al – ^{26}Mg clock.

The competing X-wind model predicts a heterogeneous distribution of ^{26}Al due to its formation by irradiation near the Sun. In this model, the Al–Mg system has no chronological significance. For example, it predicts that CAIs and chondrules formed contemporaneously in spatially distinct regions close to the young Sun, and the observed differences in their $^{26}\text{Al}/^{27}\text{Al}$ ratios reflect variable local formation of ^{26}Al by solar-induced particle irradiation. This debate can be resolved by confirming the ~ 2 Myr age difference between the formation of CAIs and chondrules that is inferred from the ^{26}Al – ^{26}Mg clock with a long-lived decay system such as the U–Pb system, since it provides ages that are free from assumptions of parent nuclide homogeneity. Connelly et al. (2008a) recently reported an age of 4565.45 ± 0.45 Myr for the formation of Allende chondrules, an age that defines an offset of 1.66 ± 0.48 Myr between the formation of CAIs and chondrules in CV chondrites. This age offset is in excellent agreement with the relative ages determined using the ^{26}Al – ^{26}Mg system for this chondrite group. This is not a prediction of the X-wind model for the origin of chondrules and CAIs, and production of ^{26}Al by solar-induced ^3He irradiation (Shu et al.,

2001; Gounelle et al., 2001), or any model of local irradiation. Instead, the results of Connelly et al. (2008a) support a stellar origin for ^{26}Al followed by injection into the nascent Solar System from stellar winds or supernova debris, requiring that our Sun formed in association with one or several massive stars.

2.1.3. ^{41}Ca – ^{41}K ($T_{1/2} \sim 0.1$ Myr)

Calcium-41 is a nuclide that can be effectively synthesized by either stellar nucleosynthesis or particle irradiation processes. If of stellar origin, the initial abundance and distribution of ^{41}Ca in early Solar System solids could provide strong constraints on the timescale and mechanism for the initiation and duration of collapse of the protosolar molecular cloud. Clear evidence for the former presence of live ^{41}Ca in the early Solar System was demonstrated by Srinivasan et al. (1996), in a detailed K isotope study of CAIs from the Efremovka meteorite that defined an initial ^{41}Ca abundance of $\sim 1.4 \times 10^{-8}$. Sahijpal et al. (1998) confirmed the former existence of ^{41}Ca in the early Solar System, and further established the presence of excess ^{41}K due to *in situ* decay of ^{41}Ca in components from other carbonaceous chondrites. Importantly, these authors demonstrated that the former presence of ^{41}Ca is correlated to that of ^{26}Al , suggesting a common source for these two nuclides and, by extension, a stellar origin for ^{41}Ca in the early Solar System.

2.1.4. ^{60}Fe – ^{60}Ni ($T_{1/2} \sim 1.5$ Myr)

Iron-60 is a neutron-rich nuclide that is difficult to produce at significant levels by irradiation processes (there are no abundant stable nuclei that can be spalled). Determining its initial abundance is important to constrain the origin of SLRs in the early Solar System. Hints of ^{60}Fe in the solar system first came from excesses of ^{60}Ni ($^{60}\text{Ni}^*$) in CAIs with an inferred initial solar system $^{60}\text{Fe}/^{56}\text{Fe}$ [$(^{60}\text{Fe}/^{56}\text{Fe})_0$] value of $\sim 1.5 \times 10^{-6}$ (Birck and Lugmair, 1988). However, the evidence that ^{60}Fe was present at time of CAI formation remains ambiguous, given the lack of correlation of $^{60}\text{Ni}^*$ values with Fe/Ni ratios and the presence of anomalies in other Ni isotopes. The first clear evidence for live ^{60}Fe in the solar system was discovered in basaltic meteorites believed to have formed at the surface of the eucrite parent body (EPB; Shukolyukov and Lugmair, 1993a,b). The initial abundance $(^{60}\text{Fe}/^{56}\text{Fe})_0 \sim 10^{-9}$ inferred from these meteorites was low enough to be consistent with an initial Solar System ^{60}Fe abundance resulting from long-term galactic nucleosynthesis (Wasserburg et al., 1996). However, this interpretation is hampered by the extended and complex thermal history of meteorites originating from the EPB (Kleine et al., 2005). Initial attempts to confirm traces of ^{60}Fe in more pristine objects such as primitive chondrite meteorites using *in situ* methods were unsuccessful (Kita et al., 2000). With continuous effort and improvement in analytical methods, clear evidence for the former presence of ^{60}Fe in chondritic components was reported in troilite and magnetite (Tachibana and Huss, 2003; Mostefaoui et al., 2005). These minerals yielded inferred $(^{60}\text{Fe}/^{56}\text{Fe})_0$ ratios ranging from $(1\text{--}1.8) \times 10^{-7}$ for sulfides from the Bishunpur and Krymka (LL3.1) chondrites

(Tachibana and Huss, 2003) to $\sim 10^{-6}$ for sulfides from Semarkona (LL3.0) (Mostefaoui et al., 2005). Given that the ^{60}Fe – ^{60}Ni systematics in sulfides can be easily disturbed by mild thermal metamorphism or aqueous alteration, recent attempts to determine the initial Solar System abundance of ^{60}Fe have focused on silicate materials (Tachibana et al., 2006). Ferromagnesian pyroxene-rich chondrules from Bishunpur and Semarkona yielded inferred $(^{60}\text{Fe}/^{56}\text{Fe})_0$ ranging from $(2.2 \pm 1.0) \times 10^{-7}$ to $(3.7 \pm 1.9) \times 10^{-7}$. By applying the time difference of 1.5–2.0 Myr between formation of these chondrules and CAIs inferred from ^{26}Al – ^{26}Mg systematics, a Solar System $(^{60}\text{Fe}/^{56}\text{Fe})_0$ of $(5\text{--}10) \times 10^{-7}$ is derived. This new estimate is inconsistent with the predicted steady state abundance of ^{60}Fe in the interstellar medium (Wasserburg et al., 1996; Harper 1996), and requires that a nearby stellar source interacted with the nascent Solar System.

Attempts to define the initial abundance of ^{60}Fe based in iron meteorites have yielded conflicting results and interpretations. Two papers have reported small resolvable anomalies in ^{60}Ni and ^{62}Ni (Bizzarro et al., 2007; Regelous et al., 2008), albeit with contrasting systematics, whereas a third study suggests the absence of Ni isotope variability in iron meteorites (Dauphas et al., in press). This highlights the challenges involved in obtaining high-precision Ni isotopes measurements using multiple collection inductively coupled plasma source mass spectrometry, and the need for improved inter-laboratory calibrations. Two recent reports (Bizzarro et al., 2007; Quitté and Markowski, 2007), however, did not find the expected excess ^{60}Ni in SAH99555, a basaltic angrite with a well-constrained Pb–Pb age of 4564.55 ± 0.16 Myr (Connelly et al., 2008b) and evidence for live ^{26}Al at the time of its crystallization (Baker et al., 2005). The lack of significant levels of ^{60}Fe at the time of accretion of the angrite parent body is inconsistent with initial Solar System ^{60}Fe estimates inferred from Bishunpur and Semarkona chondrules, suggesting decoupling in the presence of ^{26}Al and ^{60}Fe in some early formed planetesimals. This could reflect heterogeneous distribution of ^{60}Fe in the protoplanetary disk (Regelous et al., 2008) or, alternatively, a late injection of ^{60}Fe into the protoplanetary disk at a time when ^{26}Al was already homogenized (Bizzarro et al., 2007). Assuming that ^{26}Al and ^{60}Fe were injected by a single star, the late injection model suggests that ^{26}Al was delivered to the protosolar molecular cloud by the winds of a WR star prior to the supernova explosion that injected ^{60}Fe into the protoplanetary disk. If correct, this scenario places strong constraints on the nature and mass of the star that interacted with the nascent Solar System.

2.2. A supernova origin for SLRs in the early Solar System

The initial abundances and distribution of ^{26}Al , ^{41}Ca and ^{60}Fe in the early Solar System, deduced from the study of meteorites and their components, provide overwhelming evidence that they originated in a stellar nucleosynthetic source; by extension, perhaps the majority of SLRs originated this way. Current models propose that either a core-collapse supernova or a thermally pulsating asymptotic giant branch (AGB) star produced and delivered

^{60}Fe as well as other SLRs to the nascent Solar System. AGB stars, however, are old objects not associated with sites of low-mass star formation. The probability of an AGB star injecting appreciable amounts of dust in a given forming protoplanetary system is very low. AGB stars are not associated with star-forming regions. A star enters the AGB stage after at least 10 Myr of evolution. The cluster in which the star was formed has dispersed by this time. Any association between an AGB star and a star-forming region will be coincidental, and not a necessary consequence of the observed star-forming process.

Using observational data, one can estimate the probability of a protosolar system being polluted by an AGB star. Using Infrared Astronomical Satellite data, Jura and Kleinmann (1989) identified 70 high mass-loss AGB stars ($>10^{-6} M_{\odot} \text{ yr}^{-1}$) within 1 kpc of the solar system, most of them within 200 pc of the galactic mid plane. This results in an average AGB star density of $70/(\pi \times (1 \text{ kpc})^2 \times 400 \text{ pc}) \approx 10^{-8} \text{ pc}^{-3}$. Assuming these stars have peculiar velocities of 20 km s^{-1} , a value representative of the radial velocities of heavily mass-losing AGB stars within a kpc of the Sun (Kastner et al., 1993), these stars would have traveled 20 pc during their lifetime (1 Myr; Iben and Renzini, 1983). Assuming a system will be sufficiently contaminated with SLR if the AGB star passes within 1 pc of it, one calculates that $\pi \times (1 \text{ pc})^2 \times 20 \text{ pc} \approx 60 \text{ pc}^3$ will be contaminated by AGB stars. It follows that the fraction of volume in the solar neighborhood contaminated by AGB stars is $\sim 4 \times 10^{-6}$. Hence a little more than 1 part in 10^6 of the volume within 1 kpc of the sun will receive the required amount of SLRs every Myr. This basically shows that AGB injection is quite improbable. More detailed calculations were done by Kastner and Myers (1994), using the position of known AGB stars with respect to molecular clouds. They calculated the probability that some part of a large molecular cloud be contaminated by an AGB star within a 4 Myr period to be roughly 5%. However, the odds of a specific newly forming solar system are much lower, less than 3×10^{-6} per 4 Myr. This is still a generous upper limit, as Kastner and Myers (1994) only require the AGB star to pass within a few parsecs of the molecular cloud. To contaminate the solar system at the levels measured in meteorites, the AGB star would be required to pass as near as 0.1 pc (Vanhala and Boss, 2000). Simply based on the likelihood of AGB stars injecting any significant amount of fresh SLR into the solar system, this nucleosynthetic source can be ruled highly improbable. Moreover, the ^{60}Fe yield from an AGB star (Wasserburg et al., 2006) may not be sufficient to account for the Solar System initial ^{60}Fe abundance inferred from some meteorite components (i.e. Tachibana et al., 2006; Quitté et al., 2007).

On the other hand, as outlined by Hester et al. (2004) and Hester and Desch (2005), supernovae are both spatially and temporally associated with star-forming regions. Given the short lifespan of massive stars ($\sim 3\text{--}30$ Myr), it appears inevitable in this astrophysical setting that supernovae will contaminate nearby molecular clouds that are forming stars, and will pelt the majority of newly formed disks, with supernova-produced SLRs. Furthermore, supernova models can appropriately reproduce the relative abundances

of most SLRs inferred to have been present in the early Solar System (Meyer, 2005; Huss et al., 2008; see Section 4). We conclude that both meteorite studies and astronomical observations point to a nearby supernova (or more than one supernova) as the most likely source for SLRs in the young Solar System.

3. SUPERNOVA INJECTION

For supernova injection to be a viable model for the origin of the SLRs in the solar system, a causal link must exist between the explosion of a massive star and the formation of the solar system. If no such link exists and supernova injection is just happenstance, then the likelihood of the forming solar system being contaminated at the appropriate level becomes no better than if the SLR source was an AGB star. Two models linking supernova and solar system formation have been described extensively in published literature: the “Supernova Trigger” model, and the “Aerogel” model. As observations of these injection mechanisms are not possible due to the rarity of Galactic supernovae (~ 1 per century), numerical work is required to better understand and test these models. These models will be described in turn, followed by a description of the meteoritic evidence with which they are consistent.

3.1. Supernova trigger model

3.1.1. Origin of the model

Well before its past existence in meteorites was established, a stellar origin for ^{26}Al was recognized (Cameron, 1962). The discovery of evidence for the presence of the SLR ^{26}Al in chondritic refractory inclusions by Lee et al. (1976) led quickly to the suggestion that the ^{26}Al had been synthesized in a massive star, expelled during its subsequent supernova explosion, and injected into the presolar cloud by the supernova shock wave (Cameron and Truran, 1977). Because of the short half-life of ^{26}Al (0.73 Myr), it is likely that the time interval between nucleosynthesis of the ^{26}Al (assuming homogeneous distribution of ^{26}Al) and other SLRs and the formation of refractory inclusions was no more than about 1 Myr. This relatively short time interval suggested that the supernova shock front that injected the SLRs also triggered the collapse of the presolar cloud (Cameron and Truran, 1977). While the basic mechanism was suggested by Cameron and Truran (1977), their suggestion was not accompanied by modeling of the processes involved.

3.1.2. Numerical modeling

Boss (1995) was the first to present detailed three-dimensional hydrodynamics simulations of the interaction of a shock front with a target presolar cloud of solar mass, determining the conditions required for simultaneous triggering of the collapse of the cloud to protostellar densities, as well as injection of significant shock wave material into the collapsing cloud core. Boss (1995) found that only relatively slow shock fronts ($10\text{--}25\text{ km s}^{-1}$) were suitable for simultaneously triggering collapse and injection, implying that the presolar cloud core must be located at a distance

of several pc or more from the massive star, as supernova shock fronts start out with speeds of order 1000 km s^{-1} . The shock wave would be slowed down to the appropriate speed by the snowplowing of intervening dense interstellar cloud material in the several pc between the massive star and the presolar cloud core. Foster and Boss (1996) showed that the shock speed must be less than about 50 km s^{-1} in order for the shock front to be treated as a nearly isothermal gas. Higher speed shocks dissociate the molecular hydrogen necessary for cooling the post-shock gas, resulting in a more nearly adiabatic shock thermal profile, i.e. post-shock gas with temperatures roughly 100 times hotter than the pre-shock gas. Foster and Boss (1996) showed that while isothermal shocks could lead to simultaneous collapse and injection, adiabatic shocks failed to trigger collapse, and instead led to shredding and destruction of the target cloud. Foster and Boss (1997) showed that the shock wave material is injected into the presolar cloud through Rayleigh–Taylor fingers, which occur when a dense fluid (the post-shock gas) is accelerated into a less dense fluid (the target cloud). Vanhala and Boss (2000) showed that these fingers persist and become better resolved in calculations with increasingly higher spatial resolution, confirming the reality of this physical mechanism for injection. Injection can also occur if the SLRs are carried by dust grains that can be shot through the shocked gas into the target cloud (Boss, 1995), but the Rayleigh–Taylor fingers mechanism allows even post-shock gas and sub-micron dust grains carried along with the gas to be injected as well into the collapsing cloud that will form the solar system.

The highest spatial resolution models (Fig. 1, Vanhala and Boss, 2002) imply that the Rayleigh–Taylor fingers persist during the collapse down to $\sim 30\text{ AU}$ scales, where the SLRs would be injected in a spatially heterogeneous manner on the scale of the solar nebula. While these models are restricted to two spatial dimensions (axisymmetry about the vertical axis seen in Fig. 1), the fingers appear to be well resolved by the numerical code and so imply that the injection process will be spatially heterogeneous. Achieving a more homogeneous distribution of the SLRs requires rapid mixing of the SLRs (see Section 4.1). The SLRs injected into the solar nebula would be a combination of those carried along by the supernova shock front, as well as SLRs ejected from deeper shells, which have time to catch up with the slowed down leading edge of the shock and to be injected into the nebula, and isotopes that have been swept up by the intervening interstellar cloud material between the massive star and the presolar cloud. In particular, if the massive star was a W–R star that previously ejected significant ^{26}Al during its stellar wind phase, these SLRs will be swept up and injected as well. Given that ^{60}Fe is also synthesized in supernovae, this scenario can explain both the injection of ^{60}Fe from a supernova, as well as ^{26}Al derived from either the supernovae or a previous W–R star phase. The formation of the FUN inclusions, without evidence for live ^{26}Al , has been suggested to result from the formation of the first refractory solids in the nebula, prior to the somewhat delayed arrival of the first Rayleigh–Taylor fingers carrying the freshly synthesized ^{26}Al and other SLRs (Sahijpal and Goswami, 1998).

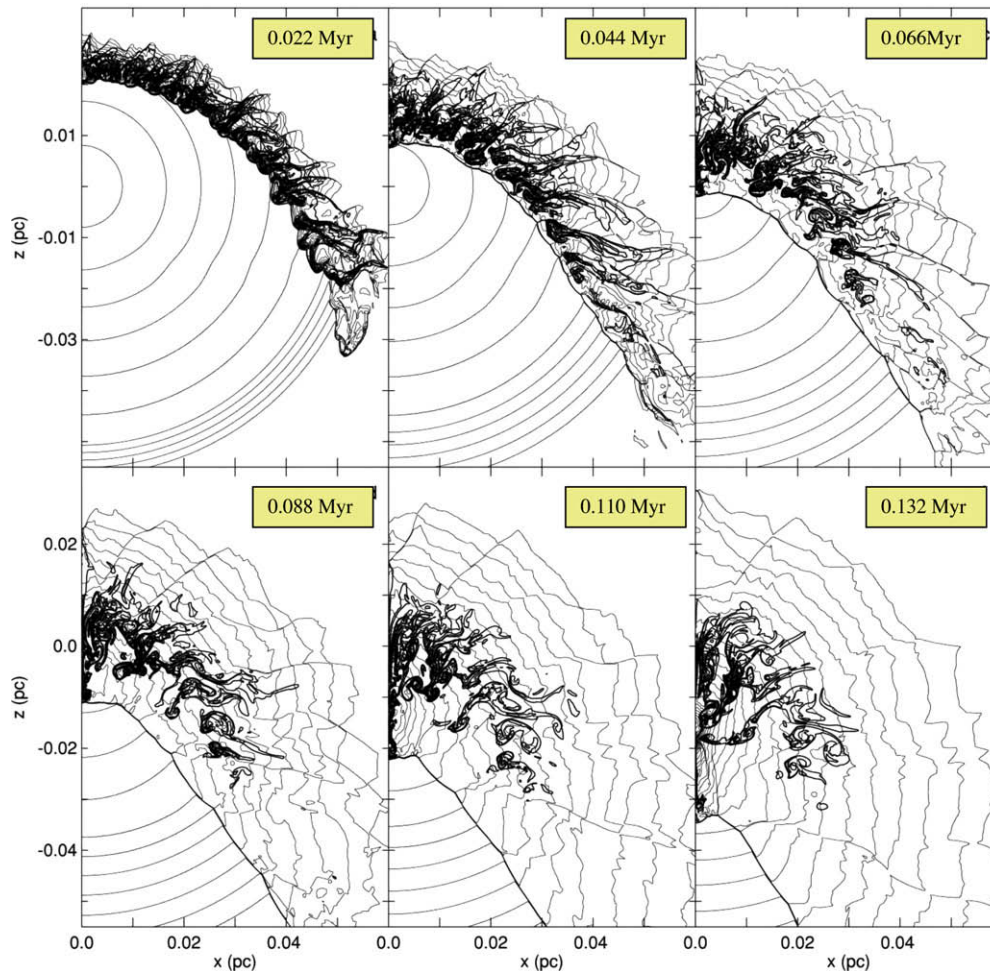


Fig. 1. Development of Rayleigh–Taylor fingers during triggered collapse of the presolar cloud (Vanhala and Boss, 2002). A 20 km s^{-1} shock front has struck the presolar cloud from above, triggering the collapse of the solar-mass cloud on the time scales shown. The thin contours represent the target cloud, while the thick contours delineate the shock front material (color field), which forms multiple well-defined fingers, allowing shock wave material to be injected into the presolar cloud and sprayed onto the surface of the solar nebula. (For interpretation of colour mentioned in this figure, the reader is referred to the web version of this article.)

It remains to be seen how the injection process will work with a fully three-dimensional cloud, and with a detailed treatment of the shock front thermodynamics. The latter point is especially germane, as Vanhala and Cameron (1998) were unable to achieve simultaneous injection and triggered collapse when they studied nonisothermal shock fronts. Extending the triggered collapse calculations all the way down to the scale of the solar nebula is another challenge for the future, in order to better understand how the disk injection and mixing processes occur and interact with each other.

3.2. Aerogel model

3.2.1. Origin of the model

Looking at images of star-forming regions like the Orion nebula (McCaughrean and O’Dell, 1996), the Carina nebula (Smith et al., 2003), or NGC 6611 (Oliveira et al., 2005), one can see low-mass stars forming in close proximity to massive stars. This is not a situation unique to these few examples;

formation of Sun-like stars is very common in massive clusters. Lada and Lada (2003) have conducted a complete census of embedded protostars within 2 kpc of the Sun and have concluded that 70–90% of protostars form in clusters. Integration of the cluster initial mass function indicates that out of all the stars born in clusters of at least 100 members, about 70% will form in clusters with at least one star massive enough to explode as a supernova (Adams and Laughlin, 2002; Hester and Desch, 2005). Hence more than 50% of low-mass stars will form in association with a supernova. As the massive star explodes, SLR-bearing ejecta will hit protoplanetary disks within a few parsecs of the supernova. If the disk survives the collision with the ejecta, some of the radioactivities may be injected, most likely in the form of dust grains (Ouellette et al., 2005). This scenario has been dubbed the “aerogel” model, as the SLRs are injected in the disk in a manner similar to interplanetary dust particles being collected in aerogel.

The likelihood of the aerogel model has been called into question recently by Williams and Gaidos (2007) and by

Gounelle and Meibom (2008). These authors conclude the probability of a disk being injected with Solar System levels of SLRs during its first 1 Myr of evolution is <1%. They base these conclusions on the improbability of a protoplanetary disk forming ~ 4 Myr after the supernova progenitor, close enough to it to receive sufficient SLRs, but not so close to be destroyed by the supernova explosion or (in the Gounelle and Meibom, 2008 paper) photoevaporation by the supernova progenitor. In fact, star formation is widely recognized to be triggered in clusters with massive stars, and to be an ongoing process (see Hester and Desch, 2005). Massive stars emit copious amounts of UV radiation that ionizes surrounding gas and drives shocks into the gas; these shocks locally and transiently increase the pressure, which triggers star formation. This obviates concerns about photoevaporation, because at typical rates of photoevaporation (e.g., $G_0 < 3 \times 10^4$, equivalent to being 1 pc from an O6 star like θ^1 Ori C, the central star in the Orion Nebula), as calculated by Adams et al. (2004), more than 4 Myr is required to strip gas down from <40 AU. Extrapolating from their results, we estimate that even at 0.3 pc from such a massive star, photoevaporation of a disk to <40 AU in a radius would take longer than the assumed age of the disk, <1 Myr. A dramatic example of this is the proplyd reported in NGC 6357 by Hester and Desch (2005), which lies ~ 0.4 pc from an O If * star, which has already evolved off the main sequence and will explode in <1 Myr. Proplyds, rapidly photoevaporating protoplanetary disks, are detectable only because they are still in the earliest stages of photoevaporation, <10⁵ yr old (Hester et al. 1996). The disk in NGC 6357 will be peppered by ejecta from a close (<0.4 pc) supernova within the first 1 Myr of its evolution. The likelihood of this event depends on the typical proximity of new disks to massive stars, determination of which awaits more complete data about the spatial distribution of triggered star formation in massive clusters, which is an active area of astronomical research. This issue is further complicated by the fact that supernova ejecta are quite clumpy, as in SN 1987A (Wooden et al., 1993) and Cas A (Fesen et al., 2006); clumps of ejecta can significantly contaminate distant disks even as nearby disks are completely missed by the ejecta. So it is premature to declare injection of SLRs into disks to be improbable.

We note in passing that it may yet be the case that injection into disks, as in the aerogel model, is something that happens to $\sim 1\%$ of disks, as calculated by Williams and Gaidos (2007) and Gounelle and Meibom (2008). Even so, this is a probability that should be compared only to other models that successfully explain the abundances of SLRs inferred from meteorites, especially ⁶⁰Fe because it cannot be produced sufficiently within the Solar System. AGB stars can produce ⁶⁰Fe, but are four orders of magnitude less probable than supernova injection into a disk. The likelihood of injection of supernova material into a molecular cloud, as in the supernova trigger model, has not been assessed. Gounelle and Meibom (2008) reject the aerogel model because of its perceived improbability, but their alternative suggestion, inheritance of ⁶⁰Fe from the interstellar medium, is not just improbable but impossible, as ⁶⁰Fe injected by supernovae into the hot phase of the inter-

stellar medium decays completely before the gas can cool and condense into molecular clouds (e.g., Harper, 1996; Wasserburg et al., 1996; Jacobsen, 2005). This is to say that improbabilities such as those calculated by Williams and Gaidos (2007) and Gounelle and Meibom (2008) are only meaningful in a comparative way, in the proper context. And as stated above, it is not yet clear whether injection into disks is as rare as they claim.

3.2.2. Disk survival

A disk sitting a few tenths of a parsec from a supernova will be hit by fast moving ejecta, travelling a few $\cdot 10^3$ km s⁻¹. Shocks of these velocities tend to shred apart molecular cloud cores (e.g., Nittmann et al., 1982), and numerical simulations show that only if the shock is substantially slowed can it compress the cloud core and trigger star formation without shredding it (Vanhala and Boss, 2000; see Section 3.1). Protoplanetary disks differ from cloud cores, however, in that they are much denser, more compact structures, thanks to the gravitational pull of the already formed protostars at their centers. The aerogel model for SLR injection is therefore viable, provided one can demonstrate that protoplanetary disks are largely resistant to shocks.

Chevalier (2000) used momentum arguments to demonstrate that disks will be partially stripped by, but will largely survive, the impact of supernova ejecta. He argued that if enough momentum from the ejecta could be transferred to gas in the disk, the resulting disk gas velocity could be greater than the local velocity of escape from the protostar, which would lead to disk destruction. Simply put, the disk may be stripped anywhere $M_{ej}V_{ej}/4\pi d^2 > \Sigma_d V_{esc}$ where M_{ej} is the ejected mass, V_{ej} is the ejecta velocity, d is the distance to the supernova, Σ_d is the surface density of the disk [$\Sigma_d = 1700 (r/1 \text{ AU})^{-1.5}$ g cm⁻² for a minimum mass disk, Hayashi et al., 1985] and V_{esc} is the escape velocity in the disk. Taking a supernova ejecting 20 M_⊙ isotropically at a $V_{ej} = 2000$ km s⁻¹, sitting 0.1 pc from a disk, calculations show that disk gas within ~ 30 AU of the central star should survive, and only material outside 30 AU would be stripped away. Comparable conclusions were reached using 1-D hydrodynamic simulations (Ouellette et al., 2005).

Recent 2-D hydrodynamic simulations have shown that disks are even more robust (Ouellette et al., 2007a). Simulations have considered a variety of distances from the supernova, explosion energies and disk masses. A snapshot of a disk being hit by ejecta can be seen in Fig. 2, and reveals effects that are not considered by Chevalier (2000) or Ouellette et al. (2005), that only manifest themselves in multidimensional calculations. First, a bow shock forms around the disk, slowing down the incoming gas and deflecting it laterally, reducing the effective momentum imparted to the disk. Second, the high pressures past the bow shock compress the disk to a smaller size, making it less vulnerable to stripping by the rapid-moving ejecta. It was found that a 40 AU disk would survive almost intact a supernova explosion 0.1 pc away, losing only 1% of its mass. However, very little gaseous ejecta are injected in the disk during this process: only about 1% of the gaseous ejecta intercepted by the disk will make its way into the disk. If the SLRs are

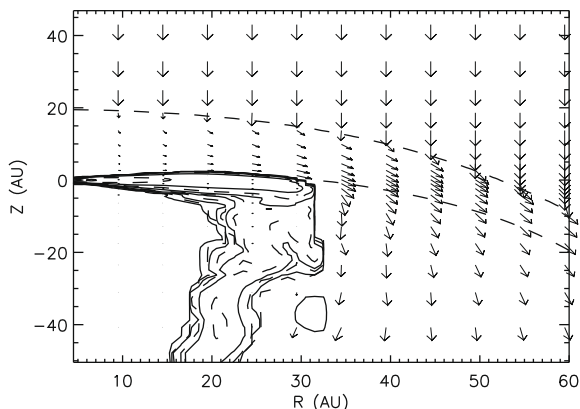


Fig. 2. Isodensity contours of protoplanetary disk being hit by ejecta. Contours are spaced a factor of 10 apart, with the outermost contour representing a density $10^{-22} \text{ g cm}^{-3}$. Contours alternate between full lines and dashed lines. The disk is substantially deformed by the high pressures in the surrounding shocked gas. Arrows indicate gas velocities as the ejecta are deviated around the disk.

found in the gas phase of the ejecta, this model fails to explain the ratios seen in meteorites by roughly two orders of magnitude.

3.2.3. Dust injection

All of the SLRs inferred from meteorites are relatively refractory elements (even Cl is only moderately volatile; Lodders, 2003). These elements should condense out of the supernova ejecta as dust grains before colliding with a disk. Colgan et al. (1994) observed the production of dust 640 days after SN 1987A, strongly suggesting that the Fe and other refractory elements did condense out of the cooling supernova ejecta, in less than 2 years. IR observations of supernova remnants detect *minimum* dust masses on the order of $10^{-4} M_{\odot}$ (Dwek et al., 1992; Wooden et al., 1993 for SN 1987A, Elmhamdi et al., 2003 for SN 1999em), or even $>10^{-2} M_{\odot}$ (Sugerman et al., 2006 for SM 2003gd; Rho et al., 2008 for Cas A). The amount of actual dust present must be higher if the ejecta are clumpy and the dust is hidden in optically thick clumps, as is commonly observed (e.g., Wooden et al., 1993 for SN 1987A). Submillimeter observations (which see into the clumps that are optically thick in the infrared) of the galactic remnants Cas A and Kepler suggest important quantities of dust could be present, up to $\sim 1 M_{\odot}$ (Dunne et al., 2003; Morgan et al., 2003).

The sizes of supernova dust grains are difficult to determine from astronomical observations. Solid-state emission features from the dust in the Cas A remnant have been observed and constrain the diameters of the dust grains to no more than $\sim 1 \mu\text{m}$ (Rho et al., 2008), but without imposing a lower limit. From studies of presolar SiC X grains (from supernovae) in the Murchison meteorites, a distribution of sizes is inferred, consistent with a log-normal distribution centered on $0.4 \mu\text{m}$ (Amari et al., 1994; Hoppe et al., 2000). Other dust grains from supernovae observed in other meteorites have similar sizes (Bernatowicz et al., 2006).

Such analyses from meteorites are necessarily restricted to particles $>0.01 \mu\text{m}$ in size, and it is certainly possible that supernovae produce smaller grains in abundance; indeed, some condensation models (e.g., Kozasa et al., 1991) tend to predict such small sizes. But we interpret the observed turnover in X grain abundance at sizes $<0.4 \mu\text{m}$ to be reflective of the size distribution of supernova dust grains. In that case, the vast majority of the mass of supernova dust resides in larger particles $\sim 1 \mu\text{m}$ in size.

Dust grains should be dynamically coupled to the supernova ejecta as they travel towards the disk. However, as they cross the bow shock, the dust grains will feel a drag force and may be deflected around the disk similarly to the gaseous ejecta. However, simple calculations show that this will not be the case. The dust trajectory can be separated into two components: its vertical motion towards the disk, and its radial motion away from the disk's axis. This radial motion will be due to the gas flowing around the disk. The drag force F on a small highly supersonic particle in a rarefied gas is given by $F \approx \pi r^2 \rho_g v_{\text{th}} \Delta v$, where r is the dust radius, ρ_g is the gas density, v_{th} is the gas thermal velocity and Δv is the velocity difference between the gas and the dust. As initially the dust has no radial velocity, Δv can be approximated by the radial velocity of the gaseous ejecta flowing around the disk. Modifying this equation to obtain a , the acceleration experienced by a dust grain, we get

$$a = \frac{\pi r^2 \rho_g v_{\text{th}} \Delta v}{\frac{4\pi}{3} \rho_s r^3} = \frac{3}{4} \frac{\rho_g v_{\text{th}} \Delta v}{\rho_s r}, \quad (1)$$

where ρ_s is density of the dust grain. The dust grain will feel this acceleration in the radial direction until it completes its vertical trajectory from the bow shock to the edge of the disk. The time taken for the dust to complete this trajectory can be approximated as $\Delta t = \Delta z / v_{\text{ej}}$, where Δz is the distance between the bow shock and the disk ($\sim 20 \text{ AU}$ according to Fig. 2), and v_{ej} is the velocity of the supernova ejecta, the dust being coupled to it ($\sim 2000 \text{ km s}^{-1}$; Ouellette et al., 2007a). In that time, the gas flowing around the disk will have deflected the dust grain a distance

$$\Delta x \approx \frac{a \Delta t^2}{2} = \frac{3}{8} \frac{\rho_g v_{\text{th}} \Delta v \Delta z^2}{\rho_s r v_{\text{ej}}^2}. \quad (2)$$

From the simulations done in Ouellette et al. (2007a), $\Delta v \sim 200 \text{ km s}^{-1}$ and $\rho_g \sim 10^{-18} \text{ g cm}^{-3}$ in the bow shock a few years after the initial collision between the ejecta and the disk. In the bow shock, the gas temperature is $\sim 10^8 \text{ K}$, resulting in a gas thermal sound speed of $v_{\text{th}} \sim 2000 \text{ km s}^{-1}$. Assuming $\rho_s \sim 2.5 \text{ g cm}^{-3}$, a density typical for silicates, the dust displacement in the radial direction can be approximated by

$$\Delta x \approx 1 \left(\frac{r}{1 \mu\text{m}} \right)^{-1} \text{ AU}. \quad (3)$$

From this simple calculation one can see that even small grains, $0.1 \mu\text{m}$ in diameter, should not be deflected more than 10 AU , and still make their way into the disk.

Of course, this is a simple calculation that assumed dust grains will not slow their vertical motion towards the disk.

In reality, gas drag will slow their velocity, and they will spend more time in the bow shock than assumed in the previous paragraphs. In addition, the dust may stop in the upper layers of the disk and be stripped away by the supernova ejecta flowing around it. Hence a numerical code was written to compute the trajectories of the dust grains as they travel through the bow shock towards the disk (Ouellette et al., 2007b). Using the gas densities and velocities computed in the Ouellette et al. (2007a) simulations, the trajectories of dust grains of 4 different sizes (10, 1, 0.1 and 0.01 μm) were followed. The drag coefficient used to compute the drag forces on the grains were taken from Gombosi et al. (1986). Their temperature is calculated using assuming a balance between drag heating (Gombosi et al., 1986) and radiative cooling. This was done for a variety of impact parameters, every 0.5 AU between 4 and 30 AU, and every year until the gaseous ejecta no longer hit the disk, 900 years after the initial contact. The dust is followed until it stops, leaves the simulation boundary, or vaporizes, when it reaches a temperature set to 1500 K. The dust grains were considered injected if they vaporized or stopped after they reached a depth in the disk where the density is greater than $10^{-16} \text{ g cm}^{-3}$, which is within 3 scale heights of the midplane. At this depth, disk processes dominate over the effect of the disk-ejecta collision, and the dust should be protected from stripping by the supernova ejecta.

The results of the computation can be found in Figs. 3 and 4. Integrating the results of the simulations over 900 years, it was found that more than 90% of the dust grains larger than 1 μm were injected. Even the smaller 0.1 μm dust grains were injected at a 70% efficiency. Only the smaller 0.01 μm dust was almost completely deflected. Using these injection efficiencies and the grain size distribution described in Amari et al. (1994), it is possible to estimate the percentage of the mass that will be injected in

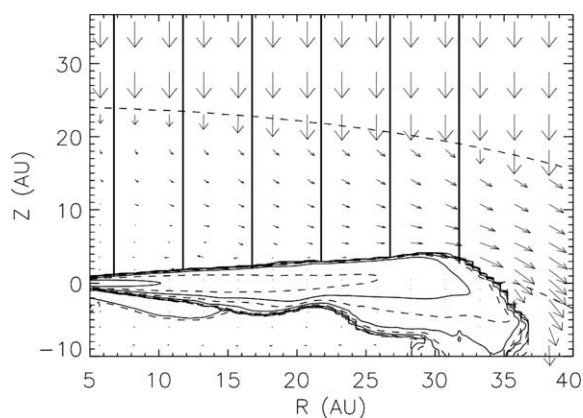


Fig. 3. Trajectories of 1 μm dust grains initially entrained in the gaseous ejecta. This figure represents a zoom in of Fig. 2, with the full and dashed lines representing the same density contours, and the arrows indicating gas velocities. The thick lines represent the trajectories of 1 μm dust grains moving towards the disk. The dust grains decouple from the gaseous ejecta as they reach the bow shock, and continue their trajectories towards the disk, in which they are efficiently injected.

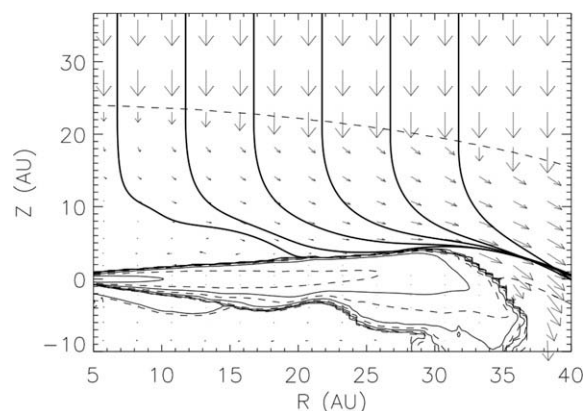


Fig. 4. Trajectories of 0.01 μm dust grains initially entrained in the gaseous ejecta. The lines and arrows are the same as in Fig. 3, except the thick lines, which now represent the trajectories of 0.01 μm dust grains. As it crosses the bow shock, the dust is deflected away from the disk, flowing around it.

the disk. On average, more than 90% of the dust mass is injected deep into the disk. If this size distribution of dust grains condensed from the supernova ejecta is similar to what is observed in meteorites, the majority of the SLRs, condensed into dust grains, should make it into the disk. Even if the average dust grain size is smaller, $\sim 0.1 \mu\text{m}$, more consistent with the size distribution of interstellar grains (Mathis et al., 1977), about 70% of the SLR bearing dust grains should be injected into the disk. The lower dust injection efficiency can be offset if the protoplanetary disk is situated closer to the supernova, intercepting a larger amount of ejecta, or if the disk is hit by a denser clump of ejecta from an inhomogeneous explosion.

3.2.4. Matching meteoritic observations

The aerogel model can easily explain the existence of FUN inclusions devoid of ^{26}Al , as the disk is already formed when the SLRs are injected, allowing ample opportunity for the first solids to form in a SLR-free environment prior to the injection. In addition, this scenario could be consistent with a decoupling of ^{60}Fe and ^{26}Al if the supernova progenitor was massive enough to enter a Wolf–Rayet phase before exploding (Bizzarro et al., 2007). During a Wolf–Rayet phase, powerful winds from the star will eject large amounts of ^{26}Al from the star; later, during the supernova proper, ^{60}Fe is ejected in the explosion. One can consider a “hybrid” model where Wolf–Rayet winds trigger the collapse of a molecular cloud core, injecting ^{26}Al in the process, and the following supernova injects the ^{60}Fe in an already formed disk. The details of this hybrid model have not yet been worked out.

4. MIXING IN THE DISK

The initial distribution of SLRs in the solar nebula is expected to be highly non-uniform, whether the SLRs are derived from supernova triggering and injection or from the aerogel scenarios. Use of SLRs such as ^{26}Al as nebula chronometers requires an initially nearly homogeneous distribu-

tion of SLRs. Mixing of these SLRs in the disk may occur on the large scale in the disk, via disk instability, or on the smaller scale, via turbulent diffusion. In this section, the physics driving these mixing mechanisms will be described, and their efficiency at mixing inhomogeneously injected SLRs in the disk will be discussed.

4.1. Disk instability

An attractive means for explaining isotopic homogenization is through the large-scale transport and mixing associated with the dynamics of a marginally gravitationally unstable disk of the type that seems to be necessary to form Jupiter by either the disk instability or core accretion mechanisms for gas giant planet formation (Boss, 2004). Three-dimensional models of the evolution of the solar nebula show that such a disk is likely to form multiple spiral arms, capable of the rapid inward transport of gas and dust to the central protostar, as well as the outward transport of angular momentum and a smaller fraction of the disk's gas and dust. SLRs injected onto the inner disk can be transported inward onto the central protostar and outward to the edge of the disk on time scales of only 1000 yr by these vigorous gravitational torques (Figs. 5 and 6).

In addition to rapid transport, marginally gravitationally unstable disk models show that the initially strongly heterogeneous distribution of newly injected SLRs are equally rapidly homogenized by the mixing accompanying the large-scale transport of the disk gas and dust. Any dust grain smaller than about 1 cm will be effectively tied to the gas during such short time scales and so can be transported over distances of 10s of AUs and homogenized to a high degree as well. The evolution of the dispersion of the number density of injected SLRs to the mean density shows that the initial heterogeneity decays to a level of homogeneity of order 10% within a few thousand years as a result of the gravitational torques (Fig. 7). This level of homogeneity and rate of homogenization appears comply with the homogeneity required for use of ^{26}Al as a chronometer and is consistent with the homogeneity observed in the three stable oxygen isotopes (Clayton and Mayeda, 1996; Boss, 2007). This mixing and transport occurs via clearly defined physical processes and appears to be a natural outcome of the same processes that lead to gas giant planet formation. It also acts independently of turbulent diffusion, but turbulent diffusion also may operate and further mix on small scales.

4.2. Turbulent diffusion and radial flows

To the extent that turbulence exists in protoplanetary disks, it seems inevitable that small grains will be diffused by the turbulence. A detailed review of the relevant processes has been given by Cuzzi and Weidenschilling (2006). The evidence for turbulence in protoplanetary disks is quite strong. Observations show that not only do protoplanetary disks accrete mass onto their central stars; in the absence of external effects (e.g., photoevaporation), disks also grow in size over time (their outer radii increase) in a manner consistent with viscous spreading (Hartmann et al., 1998; Calvet et al., 2005). Models of viscous radial

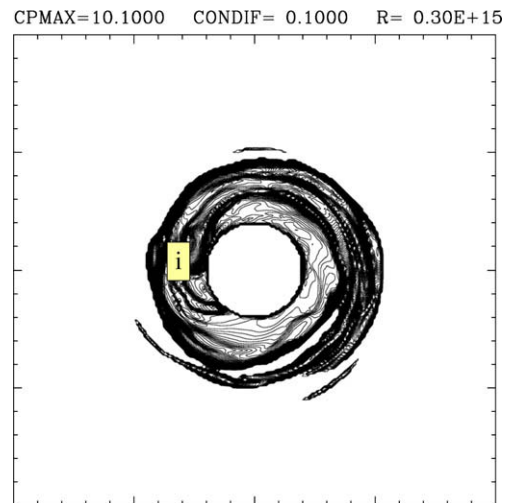


Fig. 5. Logarithmic contours of the color field density divided by the disk gas density (e.g., log of the abundance ratio $^{26}\text{Al}/^{27}\text{Al}$) in the disk midplane at a time of 227 yr after the color was sprayed onto the disk surface into a ring 90 degrees in azimuth centered on 6 AU (labeled box with “i”) from Boss (2007). Contours represent changes by factors of 1.26 up to a maximum value of 10.1, on a scale defined by the gas disk density. The region shown is 20 AU in radius with a 4 AU radius inner disk hole. The color/gas density ratio is highly non-uniform at this early phase, before the marginally gravitationally unstable disk has had a chance to transport the color field radially inward and outward and to mix the field with the disk gas. (For interpretation of colour mentioned in this figure, the reader is referred to the web version of this article.)

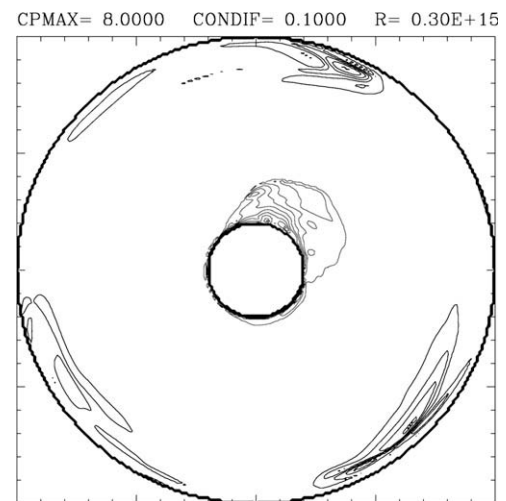


Fig. 6. Same as Fig. 5, except at a time of 3484 yr, from Boss (2007). Contours represent changes by factors of 1.26 up to a maximum value of 8.0, on a scale defined by the gas disk density. The abundances of SLR injected by a supernova are rapidly homogenized, except for inside very low gas density regions adjoining the artificial inner and outer boundaries.

spreading (e.g., Lynden-Bell and Pringle, 1974) invoke a vertically averaged turbulent viscosity parameterized as $\nu = \alpha cH$, where c is the local speed of sound, H is the local

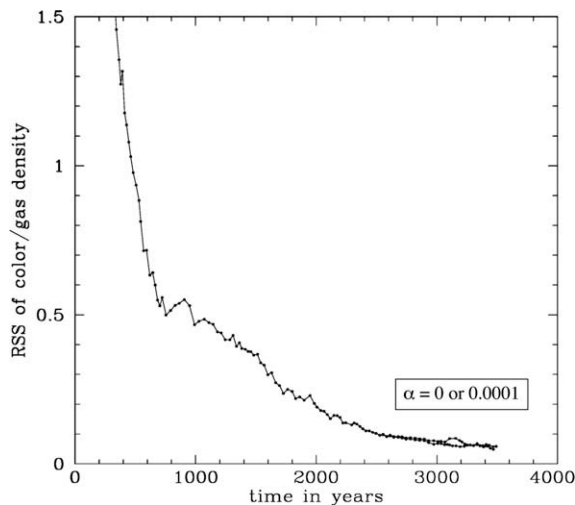


Fig. 7. Time evolution of the dispersion from the mean (i.e. standard deviation, or the root of the sum of the squares [RSS] of the differences from the mean) of the color field density divided by the gas density (e.g., $^{26}\text{Al}/^{27}\text{Al}$ abundance ratio) in the disk midplane for the model shown in Figs. 5 and 6 from Boss (2007). The color field is sprayed onto the disk surface at a time of 200 yr. Starting from high values (RSS at 200 yr is $\gg 1$), the dispersion decreases on a timescale of ~ 1000 yr and approaches a steady state value of $\sim 10\%$, independent of the presence of turbulent diffusion of the color field with respect to the gas (varied alpha values).

scale height of the disk gas, and α is a dimensionless parameter (< 1) that measures the degree of turbulent mixing and turbulent transport of angular momentum in a disk. Observations of protoplanetary disks in the Taurus Molecular Cloud suggest that $\alpha \sim 10^{-2}$, at least for disks in that region (Hartmann et al., 1998). Both gravitational instabilities and magnetorotational turbulence are consistent with this value of α . (Gammie, 1996; Gammie, 2001).

Within protoplanetary disks, the orbital velocities of annuli of gas scale as $r^{-1/2}$, so that adjacent annuli are generally sliding relative to each other; the role of turbulent viscosity is to couple these annuli so they can exchange angular momentum. As one annulus gives up angular momentum and spirals into the star, an adjacent annulus gains angular momentum and spirals outward. The total gravitational potential energy of the annuli always decreases and is dissipated as frictional heat by the viscosity, but gas can radially diffuse because the annuli are forced to spread apart radially. Because this process describes a diffusion of mass, the *net* flow of gas depends on the distribution of the mass in the disk, but is shown to be $V_r = 3(p + q - 2)v/r$, where the disk surface density falls as $\Sigma(r) \sim r^{-p}$ and the temperature falls as $T(r) \sim r^{-q}$ (Desch, 2007). If the surface distribution does not fall off too steeply with radius, then the net motion is inward, with magnitude of $1\text{--}10^2 \text{ cm s}^{-1}$ for typically assumed parameters. The typical advection timescale of SLR-bearing grains in the protoplanetary disk is therefore $\sim r/V_r \sim r^2/v$, $\sim (r/H)^2/(\alpha\Omega_K)$, where Ω_K is the Keplerian orbital frequency. Assuming $r/H \sim 20$ and $\alpha = 0.01$, the advection timescale is ~ 0.3 Myr.

Very small solids are entrained in the gas, but larger particles tend to spiral in towards the star, relative to the gas, due to gas drag. Because the gas pressure decreases with heliocentric distance, gas feels an outward force that counteracts gravity and causes it to orbit slightly slower than the Keplerian velocity (Weidenschilling, 1977). Weidenschilling (1977) calculated the inward drift rates for bodies of different sizes and found that \sim meter-sized bodies drifted inward the fastest, typically at rates equivalent to the difference in the gas orbital velocity and a Keplerian orbital velocity ($\Delta V \sim 10\text{--}100 \text{ m s}^{-1}$). For smaller particles, such as those considered here, Cuzzi and Weidenschilling have shown that the drift velocity can be approximated by $V_{\text{gd}} \sim -2St\beta V_K$ where β is $\Delta V/V_K$, which likely falls in the range of 0.001–0.01, and St is the dimensionless Stokes number, the ratio of the particle's aerodynamic stopping time $t_s = \rho_s c/\rho_g a$ (where ρ_s is the density of the solid whose radius is a , and ρ_g is the local density of gas) to the overturn timescale of the largest eddy, assumed to turn over on a time $t_L = 1/\Omega_K$. For micron-sized grains, the gas drag induced velocity is $< 1 \text{ cm s}^{-1}$, meaning it would take nearly 10 Myr to travel inward 30 AU. These timescales are reduced, however, as micron-sized grains are incorporated into larger particles, decreasing to $\sim 10^3$ years for meter-sized bodies.

In addition to being advected in an average sense, the distribution of grains within the disk will also diffuse because of the turbulence. Diffusive transport of gas and of solids entrained in the gas is a distinct process from angular momentum transport and the net motion of the gas. The coefficient parameterizing the diffusion of gas is $D = (Sc)^{-1} v$, where Sc is called the Schmidt number; it is a dimensionless number of order unity, but is not identical to 1, and must be computed for each mechanism considered. If the turbulence is due to the magnetorotational instability, computer simulations show $Sc = 4.6 \alpha^{0.26}$ for diffusion in the radial direction, and $Sc = 23.5 \alpha^{0.46}$ for diffusion in the vertical direction (Johansen et al., 2006). However, for $\alpha = 0.01$, this implies Schmidt numbers on the order of 1.5–3, and the timescale for diffusion, $\sim r^2/D$, is comparable to the timescale for advection. Very small particles are dynamically well coupled to the gas and diffuse equally fast, but larger particles diffuse more slowly. The diffusivity of dust particles is $D/(1 + St)$. This reduction in diffusivity is important for larger particles, but for micron-sized SLR-bearing supernova grains considered here, $St \ll 1$, and diffusion and advection work equally fast, on \sim Myr timescales.

Radial advection, especially in the one-dimensional picture considered above, more or less preserves compositional gradients in the disk and is not expected to homogenize material. Diffusion, on the other hand, will mix material on scales comparable to the sizes of the turbulent eddies doing the mixing. To first order, turbulent diffusion can be considered to mix dust efficiently in the nebula on timescales $\sim 0.3 \text{ Myr} (\alpha/0.01)^{-1}$ Myr. Several caveats must be kept in mind, however. Gas drag will radially sort grains of different sizes; growth of particles will greatly complicate the analysis. Exchange between solids and gas will also be significant. Ciesla and Cuzzi (2006) explicitly modeled the

combined effects of diffusion, advection, particle growth, and gas drag migration of water-bearing species in an evolving protoplanetary disk. It was found that the combined action of all these processes would lead to large-scale mixing, but that radial gradients in the concentrations of water developed that varied with time. Whether such gradients would be recorded in the chondritic meteorites or planetesimals would depend on how the timescale for the formation of these bodies or their components compared to the transport times identified above. If the formation timescale was short, then these bodies would be more likely to record concentration gradients, whereas longer formation timescales would likely record a more uniform, homogenized nebula. What is clear from this analysis is that radial mixing is not straightforward to understand.

An additional complication is worth noting. Thus far mixing calculations have largely considered one-dimensional (radial) models for mixing in the solar nebula. Recently, Ciesla (2007) demonstrated the importance of considering the vertical structure of the nebula when looking at large-scale radial mixing. Because the gas properties (density, pressure and their respective gradients) vary with height above the disk midplane, the viscous stresses and the interactions of the solids with the gas are expected to not only vary with radial distance from the star, but also vertical location as well. If one makes the simplifying assumption that Reynolds stress scales as the local gas pressure times a uniform α , it is possible to show that material would be transported outward along the midplane more efficiently than recognized in previous models, whereas inward transport is more efficient along the surfaces at high altitudes. Given that the injected material will likely come to rest 3-4 scale heights above the disk midplane, this suggests that delivery of injected material to the inner solar system could be more rapid than the timescales quoted above.

Turbulent diffusion is likely to mix SLRs throughout the disk very effectively, on short timescales (~ 0.3 Myr), but quantification of this mixing requires much additional work and a better understanding of the causes of turbulence in disks.

5. INJECTED SLRS AND EXPECTED ABUNDANCES

5.1. SLRs abundances

Incorporation of fresh stellar matter into the solar cloud or the Sun's protoplanetary disk will alter pre-existing isotopic abundances. We typically may write

$$\frac{N_i}{N_j} \approx \frac{A_j f M_i^{(ej)} e^{-\lambda_i \Delta}}{A_i M^{(0)} X_j} \quad (4)$$

Here, N is the abundance of a given species, f is the fraction of bulk supernova ejecta that is incorporated into the disk, $M^{(ej)}$ is the mass of a species in the ejecta that can be incorporated into the Solar System, $M^{(0)}$ is the mass of pre-injection material, λ is the decay rate, Δ is the decay interval and X is the mass fraction of a species. The subscripts i and j denote different species. As an example, we consider the $^{26}\text{Al}/^{27}\text{Al}$ system. We take isotope i to be ^{26}Al and isotope j to be ^{27}Al . The Solar System mass fraction of ^{27}Al is

5.80×10^{-5} (Lodders, 2003). For discussion, we consider the case in which the bulk ejecta from a well-known 25 solar mass stellar model (Meyer et al., 1995) are solely responsible for the short-lived radioactivities in the early Solar System. In this model, the bulk ejecta contain 10^{-4} solar masses of ^{26}Al . To explain the canonical ratio 5×10^{-5} in early Solar System minerals (MacPherson et al., 1995), then, we require that a fraction

$$f = 2.8 \times 10^{-5} \times M^{(0)} \times e^{0.97\Delta} \quad (5)$$

(where Δ is in Myr) of the 23.5 solar masses of ejecta mix in with the $M^{(0)}$ solar masses of pre-incorporation material. If $M^{(0)} = 1$ solar mass and $\Delta = 1$ Myr, we find $f = 7.4 \times 10^{-4}$. This suggests a fraction $F = 1.7 \times 10^{-3}$ of the Solar System's mass came from the last incorporation event. If the stellar matter were incorporated into a 0.01 solar mass protoplanetary disk after formation of the Sun, $f = 7.4 \times 10^{-6}$ with a 1 Myr decay interval. In this case again, a fraction $F = 1.7 \times 10^{-3}$ of disk matter is due to the late incorporation of matter.

Although the picture of injection of a fraction of the bulk ejecta from a massive star provides an order of magnitude estimate of the abundance effects we can expect, it is not a particularly plausible model. It is certainly more likely that only certain stellar layers get injected into the Solar cloud or protoplanetary disk either due to hydro-dynamical processes in the stellar outflow or the injection event or to preferential injection of particular chemical forms of the stellar ejecta. The simplest elaboration is to consider that only the stellar layers outside an injection "mass cut" can be incorporated into the early Solar System. Such a mass cut is plausible on physical grounds since the outer stellar layers are the most likely to be injected; however, its presence has also been suggested to avoid injection of too much ^{53}Mn into the early Solar system (Cameron et al., 1995; Meyer and Clayton, 2000; Meyer, 2005).

More complex models have been suggested in an attempt to better match the ratios predicted from supernova injection to the ones measured in meteorites. The use of a supernova with mixing-fallback, where the inner region of the exploding star experience mixing, then a fraction of this material gets ejected while the rest undergoes fallback onto the core, has been suggested as a way to better match the meteoritic abundances (Takigawa et al., 2007; Miki et al., 2007; Tachibana et al., 2007). Agreement to within a factor of 3 can be reached for ^{26}Al , ^{41}Ca , ^{53}Mn , and ^{60}Fe with this type of supernova.

Recent work by Ellinger et al. (2007) goes beyond a single mass cut used in previous models in an attempt to simulate the effect of inhomogeneous mixing of the ejecta. Instead of using a single mass cut to delimitate the boundary between material ejected in the explosion and material falling back on the star, the model uses three different mass cuts, separating three different shells. The position of these mass cuts and the relative amount of each shell injected in the disk is computed to best fit the observed SLR ratios. The results of these calculations can be seen in Table 2. Most of the ratios predicted by the computation match the adopted abundances to within 10%, demonstrating that a single supernova can plausibly explain the abundances observed in meteorites.

5.2. Stable isotopic anomalies

We now consider the possible stable isotopic anomalies that might arise from an inhomogeneous incorporation of fresh stellar matter into the Solar System. If some Solar System body (for example, the Sun itself, a meteorite parent body, or simply a primitive mineral later incorporated into a larger object) formed out of pre-injection matter, it would have an isotopic anomaly with respect to Solar System average material, which arises from the mixture. The resulting anomaly would have the magnitude

$$\begin{aligned} \delta(i, j) &= \left[\frac{(N_i/N_j)_{\text{sample}}}{(N_i/N_j)_{\text{solar}}} - 1 \right] \times 1000 \\ &= \left[\frac{f(O_j - O_i)}{1 - FO_j} \right] \times 1000 \end{aligned} \quad (6)$$

where F is the fraction of the final mass of the mixture contributed by the stellar matter and $O_i = X_i^{(\text{ej})}/X_i$ is the overabundance of species i in the fresh stellar ejecta incorporated into the Solar System using per mil notation. To get some idea about the magnitude of such anomalies, we consider injection of a fraction of the bulk ejecta from the 25 solar mass model discussed above (Meyer et al., 1995). For a time delay of 1 Myr, the f required to explain the early Solar System abundance of ^{26}Al was found to be 1.7×10^{-3} . From the same stellar model, we would expect bulk overabundances of ^{16}O and ^{17}O of 14.4 and 10.5, respectively with respect to solar system abundances (Lodders, 2003). Should one find a sample composed of purely pre-mixed material, the expected anomaly in oxygen would be $\delta^{17}\text{O} = +6.9$ per mil. A stable isotope anomaly of this magnitude is certainly observable, and the lack of such anomalies in meteoritic materials has been used to argue against an inhomogeneous distribution of short-lived radioactivities arising from injection of fresh stellar matter to explain the abundance of ^{26}Al in the early Solar System. More recently the possible presence of such anomalies in oxygen in the Sun relative to meteorites has been suggested as a possible test of the model of injection of short-lived radioactivities into the protoplanetary disk (Gounelle and Meibom, 2007).

The use of oxygen isotope anomalies as a test of injection models is, unfortunately, complicated by many factors, not least of which is the discovery of pristine pre-injection samples. Even if such samples were found and an isotopic

shift measured, it would be difficult to disentangle the isotopic shifts from mixing from other chemical isotopic fractionation processes. It is not even clear what isotopic shift should accompany injection of short-lived species into the solar cloud or protoplanetary disk, as we now discuss.

First, the predicted stable isotope anomalies will certainly depend on which stellar layers are injected. With exceptions for certain key isotopes like ^{17}O , the degree of production of isotopes in a star is most pronounced in the innermost layers and decreases outward. Injection of only the outermost layers would thus result typically in smaller anomalies than would result from injection of a fraction of the bulk ejecta (Nichols et al., 1999a). This is not true for ^{17}O for the 25 solar mass model discussed above, however, since the largest overabundance of ^{17}O is in the outer envelope. Indeed, the predicted ^{17}O anomaly becomes $\delta(^{17}\text{O}/^{18}\text{O}) = -25$ per mil if only the outer stellar envelope is injected.

The second caution is that abundance yields from stellar models have uncertainties due to uncertainties in the input physics for the models, and these can have significant effects on the resulting predictions of stable isotope anomalies accompanying injection of fresh stellar matter. For example, the cross sections for reactions on ^{17}O have been revised (Angulo et al., 1999; Blackmon et al., 1995) over the last ten years leading to nearly ten-fold reductions of the yields of ^{17}O from models of massive stars (Limongi et al., 2000; Rauscher et al., 2002). On the other hand, the cross sections for reactions governing the ^{16}O abundance were on firmer ground, so the massive star ^{16}O yields have not changed much. As a consequence, the improved nuclear physics input to the stellar models leads to a four-fold increase in the expected $^{17}\text{O}/^{16}\text{O}$ anomaly arising from an inhomogeneous distribution of short-lived radioactivities in the early Solar System if we assume injection of bulk stellar ejecta. If we instead assume injection of only the outer envelope of the star, however, the anomaly drops from -25 per mil to about -1 per mil because the outer layers in massive stars are now little enriched in ^{17}O and only slightly depleted in ^{16}O .

Another caveat is the possible discrepancy between the initial composition of the stellar models and that of the pre-injection cloud or disk composition. The stellar model yields we use are from models that begin with a solar abundance distribution. The Solar abundance distribution, however, is a result of the mixture of stellar debris and the pre-injection cloud or disk, so we would not in general expect the injecting star to start with this particular mixed composition. This discrepancy is not typically a problem for the question of the short-lived radioactivities because the cloud or protoplanetary disk did not contain much of the short-lived species prior to the injection and the abundance of the reference stable isotope is only altered a small amount by the incorporation of fresh stellar matter. For stable isotopes, however, the effect can be important.

One approach to addressing this inconsistency is to redefine the solar composition to be that resulting from the mixture of pre-injection matter, which can be taken to have the solar composition, and fresh stellar debris. The overabundances O_i then are to be computed from the post-mixture

Table 2
SLR ratio using an optimal mix of shells.

Ratio	Adopted value	Predicted value
$^{26}\text{Al}/^{27}\text{Al}$	4.5×10^{-5}	4.1×10^{-5}
$^{36}\text{Cl}/^{35}\text{Cl}$	3.0×10^{-6}	3.3×10^{-6}
$^{41}\text{Ca}/^{40}\text{Ca}$	1.4×10^{-8}	1.5×10^{-8}
$^{53}\text{Mn}/^{55}\text{Mn}$	2.0×10^{-5}	2.0×10^{-5}
$^{60}\text{Fe}/^{56}\text{Fe}$	1.0×10^{-6}	9.3×10^{-7}
$^{107}\text{Pd}/^{108}\text{Pd}$	5.0×10^{-5}	7.2×10^{-5}
$^{182}\text{Hf}/^{180}\text{Hf}$	1.1×10^{-4}	1.5×10^{-4}

Injecting ejecta from a $21 M_{\odot}$ supernova (Rauscher et al., 2002) into a solar composition disk (Lodders, 2003) ($\Delta = 0.8$ Myr).

mass fractions. This aligns the initial compositions of the star and the cloud or disk.

Nevertheless, the effect of systematic errors in the input to the stellar models remains. There is no guarantee that the solar abundance distribution used as the starting composition in the above procedure is consistent with the stellar models. In particular, we know that it is not possible to reproduce the solar abundance distribution with Galactic chemical evolution models and current stellar model yields (Nichols et al., 1999b; Timmes et al., 1995).

An approach to handling the stellar model errors is to run a chemical evolution model of the Galaxy. This procedure provides a proxy composition into which we can mix the fresh stellar debris (Nichols et al., 1999a). The idea is that systematic errors in the input to the stellar models will appear in both the composition of the pre-injection cloud or disk and in the stellar ejecta. This “normalization” procedure helps provide a more realistic estimate of the magnitude of stable isotope anomalies accompanying injection of fresh stellar matter; however, one must recognize that it can introduce its own errors (Meyer et al., 1999), and the discrepancy between the initial compositions of the disk or cloud and that of injecting star remains.

The ideal procedure for estimating the magnitude of stable isotope anomalies arising from an inhomogeneous distribution of fresh stellar ejecta in the early Solar System is a bootstrapping Galactic chemical evolution model that computes the yields for the next generation of stars from those in the current generation. Unfortunately, this is probably several years away. Until these models are available, we should continue to keep in mind the subtleties that exist in our estimates of stable isotope anomalies from injection of fresh stellar matter.

6. CONCLUSION

Short-lived radionuclides provide an important window into the past of the Solar System. They can be used to time events in the early Solar System, provided that their abundances were determined by an event with a finite extent in time, and that their abundances were uniform throughout the protoplanetary disk. These requirements are predictions of two models for the origins of SLRs. One, the supernova trigger model, hypothesizes that a local supernova triggered the collapse of the Sun’s molecular cloud core at the same time it injected radionuclides into it. The other, the aerogel model, hypothesizes that the Solar System disk had already formed when it was pelted by dust grains from a supernova <1 pc away. In each model, the injection of SLRs occurs rapidly and before most of the disk’s evolution.

Both models are consistent with the finite temporal extent of the injection. This is to be compared to models in which SLRs are continuously created over the lifetime of the disk, such as the X-wind model (Gounelle et al., 2001). Both models are also consistent with the existence of FUN inclusions, which contain no ^{26}Al , and presumably formed before the injection. Both models are also potentially consistent with homogenization within the disk. Both turbulent diffusion and gravitational instabilities can homogenize SLRs within disks on rapid timescales, $\sim 10^5$

years or less. Better quantification of the rates of homogenization will require a more complete understanding of the processes at play in disks. It has not yet been established that protoplanetary disks are gravitationally unstable or are subject to the magnetorotational instability; however, observations of viscous spreading of disks suggests one or both of these mechanisms operates in protoplanetary disks.

An origin of SLRs in supernova ejecta is consistent not only with the rough magnitude of the SLR abundances, but with the relative proportions of SLRs as well. If only material outside of a given “mass cut” is injected, the relative proportions of all the SLRs (except ^{10}Be , which has a separate origin) are reproduced to within factors of 2 or so. Of course, imaging of actual supernovae show that the explosions are highly anisotropic and clumpy. By injecting varying proportions of ejecta from three distinct regions in the supernova, the SLR abundances can be reproduced to within 10%, which rivals the accuracy of the meteoritic measurements.

The injection of SLRs will lead to “collateral damage”, as anomalous abundances of stable isotopes will be injected as well. The lack of an observed anomaly in $\Delta^{17}\text{O}$ has been invoked as evidence against supernova injection by Gounelle and Meibom (2007). However, observations of supernovae show that not all layers of the supernova will be injected into the solar nebula with equal efficiency. Moreover, the extent of the stable isotopic anomalies within the ejecta is difficult to calculate, due to uncertainties in reaction rates. Depending on the details of the injection of supernova material, no anomaly in $\Delta^{17}\text{O}$ need accompany injection of other SLRs like ^{26}Al .

In conclusion, theoretical models of injection and mixing show that SLRs in supernova ejecta can easily be injected into the solar nebula – either through triggering of the collapse of the Sun’s cloud core, or by injection into the disk. Homogenization is rapid. The use of SLRs as chronometers appears justified. The existence of SLRs like ^{26}Al and ^{60}Fe points to the Sun’s birthplace as being in the neighborhood of a massive star that exploded as a supernova.

ACKNOWLEDGMENTS

We thank the organizers of the Workshop on the Chronology of Meteorites and the Early Solar System for a very successful meeting. We thank the reviewers for comments that improved the quality of this paper.

REFERENCES

- Adams F. C. and Laughlin G. (2001) Constraints on the birth aggregate of the solar system. *Bull. Am. Astron. Soc.* **34**, 941.
- Amari S., Lewis R. S. and Anders E. (1994) Interstellar grains in meteorites. I – isolation of SiC, graphite, and diamond; size distributions of SiC and graphite. II – SiC and its noble gases. *Geochim. Cosmochim. Acta* **58**, 459–470.
- Angulo C. et al. (1999) A compilation of charged-particle induced thermonuclear reaction rates. *Nucl. Phys.* **656**, 3–183.
- Baker J., Bizzarro M., Wittig N., Connelly J. and Haack H. (2005) Early planetesimal melting from an age of 4.5662 Gyr for differentiated meteorites. *Nature* **436**, 1127–1131.

- Baker R. G. A., Schönbachler M. and Rehkämper M. (2007) New evidence from carbonaceous chondrites for the presence of Live ^{205}Pb in the early solar system. *Lunar Planet. Sci.* **XXXVIII**, 1840.
- Bernatowicz T. J., Croat T. K. and Daulton T. L. (2006) Origin and evolution of carbonaceous presolar grains in stellar environments. In *Meteorites and the Early Solar System II* (eds. D. S. Lauretta and H. Y. McSween Jr.). University of Arizona Press, Tucson, pp. 109–126.
- Birck J. L. and Lugmair G. W. (1988) Nickel and chromium isotopes in Allende inclusions. *Earth Planet. Sci. Lett.* **90**, 131–143.
- Bizzarro M., Baker J. A. and Haack H. (2004) Mg isotope evidence for contemporaneous formation of chondrules and refractory inclusions. *Nature* **431**, 275–278.
- Bizzarro M., Baker J. A., Haack H. and Lundgaard K. L. (2005) Rapid timescales for accretion and melting of differentiated planetesimals inferred from ^{26}Al – ^{26}Mg chronometry. *Astrophys. J.* **632**, L41–L44.
- Bizzarro M., Ulfbeck D., Trinquier A., Thrane K., Connelly J. N. and Meyer B. S. (2007) Evidence for a late injection of ^{60}Fe into the protoplanetary disk. *Science* **316**, 1178–1181.
- Blackmon J. C., Champagne A. E., Hofstee M. A., Smith M. S., Downing R. G. and Lamaze G. P. (1995) Measurement of the ^{17}O , α ^{14}N cross section at stellar energies. *Phys. Rev. Lett.* **74**, 2642–2645.
- Boss A. P. (1995) Collapse and fragmentation of molecular cloud cores. II. Collapse induced by stellar shock waves. *Astrophys. J.* **439**, 224–236.
- Boss A. P. (2004) Evolution of the solar nebula. VI. Mixing and transport of isotopic heterogeneity. *Astrophys. J.* **616**, 1265–1277.
- Boss A. P. (2007) Evolution of the solar nebula. VIII. Spatial and temporal heterogeneity of short-lived radioisotopes and stable oxygen isotopes. *Astrophys. J.* **660**, 1707–1714.
- Calvet N., Briceño C., Hernández J., Hoyer S., Hartmann L., Sicilia-Aguilar A., Megeath S. T. and D'Alessio P. (2005) Disk evolution in the Orion OB1 Association. *Astron. J.* **129**, 935–946.
- Cameron A. G. W. (1962) Formation of the solar nebula. *Icarus* **1**, 339–342.
- Cameron A. G. W. and Truran J. W. (1977) The supernova trigger for formation of the Solar System. *Icarus* **30**, 447–461.
- Cameron A. G. W., Hoefflich P., Myers P. C. and Clayton D. D. (1995) Massive supernovae, Orion gamma rays, and the formation of the solar system. *Astrophys. J.* **447**, L53.
- Chaussidon M., Robert F. and McKeegan K. D. (2006) Li and B isotopic variations in an Allende CAI: Evidence for the in situ decay of short-lived ^{10}Be and for the possible presence of the short-lived nuclide ^7Be in the early solar system. *Geochim. Cosmochim. Acta* **70**, 224–245.
- Chevalier R. A. (2000) Young circumstellar disks near evolved massive stars and supernova. *Astron. J.* **538**, 151–154.
- Ciesla F. J. (2007) Outward transport of high-temperature materials around the midplane of the solar nebula. *Science* **318**, 613–615.
- Ciesla F. J. and Cuzzi J. N. (2006) The evolution of the water distribution in a viscous protoplanetary disk. *Icarus* **181**, 178–204.
- Clayton R. N. and Mayeda T. K. (1996) Oxygen isotope studies of achondrites. *Geochim. Cosmochim. Acta* **60**, 1999–2017.
- Colgan S. W. J., Haas M. R., Erickson E. F., Lord S. D. and Hollenbach D. J. (1994) Day 640 infrared line and continuum measurements: dust formation in SN 1987A. *Astron. J.* **427**, 874–888.
- Connelly J. N., Amelin Y., Krot A. N. and Bizzarro M. (2008a) The solar system's oldest solids. *Astrophys. J.* **675**, L121–L124.
- Connelly J. N., Bizzarro M., Thrane K. and Baker J. (2008b) The U–Pb age of SAH99555 revisited. *Geochim. Cosmochim. Acta* **72**, 4813–4824.
- Cuzzi J. N. and Weidenschilling S. J. (2006) Particle-gas dynamics and primary accretion. In *Meteorites and the Early Solar System II* (eds. D. S. Lauretta and H. Y. McSween). University of Arizona Press, Tucson, pp. 353–381.
- Dauphas N., Cook D. L., Sacarabany A., Frohlich C., Davis A. M., Pourmand A., Rauscher T. and Gallino R. (2008) Iron-60 evidence for early injection and efficient mixing of stellar debris in the protosolar nebula. *Astrophys. J.* **686**, 560–569.
- Desch S. J. (2007) Mass distribution and planet formation in the solar nebula. *Astrophys. J.* **671**, 878–893.
- Desch S. J., Connolly H. C. and Srinivasan G. (2004) An interstellar origin for the beryllium 10 in calcium-rich, aluminum-rich inclusions. *Astrophys. J.* **602**, 528–542.
- Dunne L., Eales S., Ivison R., Morgan H. and Edmunds M. (2003) Type II supernovae as a significant source of interstellar dust. *Nature* **424**, 285–287.
- Dwek E., Moseley S. H., Glaccum W., Graham J. R., Loewenstein R. F., Silverberg R. F. and Smith R. K. (1992) Dust and gas contributions to the energy output of SN 1987A on day 1153. *Astron. J.* **389**, L21–L24.
- Ellinger C. I., Desch S. J. and Ouellette N. (2007) A core-collapse supernova as the source of short-lived radionuclides in the solar system. *Meteorit. Planet. Sci. Suppl.* **42**, 5121.
- Elmhamdi A. et al. (2003) Photometry and spectroscopy of the Type IIP SN 1999em from outburst to dust formation. *Mon. Not. R. Astron. Soc.* **338**, 939–956.
- Fahey A., Zinner E. and MacPherson G. (1987) Where do hibonites with anomalous Ti and no excess ^{26}Mg come from? *Meteoritics* **22**, 377.
- Fesen R. A. et al. (2006) The expansion asymmetry and age of the Cassiopeia A supernova remnant. *Astrophys. J.* **645**, 283–292.
- Foster P. N. and Boss A. P. (1996) Triggering star formation with stellar ejecta. *Astrophys. J.* **468**, 784–796.
- Foster P. N. and Boss A. P. (1997) Injection of radioactive nuclides from the stellar source that triggered the collapse of the presolar nebula. *Astrophys. J.* **489**, 346–357.
- Gammie C. F. (1996) Layered accretion in T Tauri disks. *Astrophys. J.* **457**, 355–362.
- Gammie C. F. (2001) Nonlinear outcome of gravitational instability in cooling, Gaseous Disks. *Astrophys. J.* **553**, 174–183.
- Gombosi T. I., Nagy A. F. and Cravens T. E. (1986) Dust and neutral gas modeling of the inner atmospheres of comets. *Rev. Geophys.* **24**, 667–700.
- Gounelle M. (2006) The origin of short-lived radionuclides in the solar system. *New Astron. Rev.* **596**, 596–599.
- Gounelle M. and Meibom A. (2007) The oxygen isotopic composition of the sun as a test of the supernova origin of ^{26}Al and ^{41}Ca . *Astrophys. J.* **664**, L123–L125.
- Gounelle M. and Meibom A. (2008) The origin of short-lived radionuclides and the astrophysical environment of solar system formation. *Astrophys. J.* **680**, 781–792.
- Gounelle M., Shu F. H., Shang H., Glassgold A. E., Rehm K. E. and Lee T. (2001) Extinct radioactivities and protosolar cosmic rays: self-shielding and light elements. *Astrophys. J.* **548**, 1051–1070.
- Harper C. L. (1996) Astrophysical site of the origin of the solar system inferred from extinct radionuclide abundances. *Astrophys. J.* **466**, 1026–1038.
- Hartmann L., Calvet N., Gullbring E. and D'Alessio P. (1998) Accretion and the evolution of T Tauri disks. *Astrophys. J.* **495**, 385–401.

- Hayashi C., Nakazawa K. and Nakagawa Y. (1985) Formation of the solar system. In *Protostars and Planets II* (eds. D. C. Black and M. S. Matthews). University of Arizona Press, Tucson, pp. 1100–1153.
- Hester J. J. and Desch S. J. (2005) Understanding our origins: star formation in HII region environments. In *Chondrites and the Protoplanetary Disk* (eds. A. N. Krot, E. R. D. Scott and B. Reipurth). Astronomical Society of the Pacific, San Francisco, pp. 107–132.
- Hester J. J., Desch S. J., Healy K. R. and Leshin L. A. (2004) The cradle of the solar system. *Science* **304**, 1116–1117.
- Hoppe P., Strebel R., Eberhardt P., Amari S. and Lewis R. S. (2000) Isotopic properties of silicon carbide X grains from the Murchison meteorite in the size range 0.5–1.5 μm . *Meteorit. Planet. Sci.* **35**, 1157–1176.
- Huss G. R., Meyer B. S., Srinivasan B., Goswami J. N. and Sahijpal S. (2008) Stellar sources of the short-lived radionuclides in the early solar system. *Geochim. Cosmochim. Acta* **73**, 4922–4945.
- Iben, Jr., I. and Renzini A. (1983) Asymptotic giant branch evolution and beyond. *Ann. Rev. Astron. Astrophys.* **21**, 271–342.
- Jacobsen S. B. (2005) The birth of the solar system in a molecular cloud: Evidence from the isotopic pattern of short-lived nuclides in the early solar system. In *Chondrites and the Protoplanetary Disk* (eds. A. N. Krot, E. R. D. Scott and B. Reipurth). Astronomical Society of the Pacific, San Francisco, pp. 548–557.
- Jacobsen B., Yin Q.-Z., Moynier F., Amelin Y., Krot A. N., Nagashima K., Hutcheon I. D. and Palme H. (2008) ^{26}Al – ^{26}Mg and ^{207}Pb – ^{206}Pb systematics of Allende CAIs: canonical solar initial $^{26}\text{Al}/^{27}\text{Al}$ ratio reinstated. *Earth Planet. Sci. Lett.* **272**, 353–364.
- Johansen A., Klahr H. and Mee A. J. (2006) Turbulent diffusion in protoplanetary discs: the effect of an imposed magnetic field. *Mon. Not. R. Astron. Soc.* **370**, L71–L75.
- Jura M. and Kleinmann S. G. (1989) Dust-enshrouded asymptotic giant branch stars in the solar neighborhood. *Astrophys. J.* **341**, 359–366.
- Kastner J. H. and Myers P. C. (1994) An observational estimate of the probability of encounters mass-losing evolved stars and molecular clouds. *Astrophys. J.* **421**, 605–614.
- Kastner J. H., Forveille T., Zuckerman B. and Omont A. (1993) Probing the AGB tip – luminous carbon stars in the Galactic plane. *Astron. Astrophys.* **275**, 163.
- Kita N. T., Nagahara H., Togashi S. and Morshita Y. (2000) A short duration of chondrule formation in the solar nebula: evidence from Al-26 in Semarkona ferromagnesian chondrules. *Geochim. Cosmochim. Acta* **64**, 3913–3922.
- Kita N. T., Huss G. R., Tachibana S., Amelin Y., Nyquist L. E. and Hutcheon I. D. (2005) Constraints on the origin of chondrules and CAIs from short-lived and long-lived radionuclides. In *Chondrites and the Protoplanetary Disk* (eds. A. N. Krot, E. R. D. Scott and B. Reipurth). Astrophysical Society of the Pacific, San Francisco, pp. 558–587.
- Kleine T., Mezger K., Palme H., Scherer E. and Munker C. (2005) The W isotope composition of eucrite metals: constraints on the timing and cause of the thermal metamorphism of basaltic eucrites. *Earth Planet. Sci. Lett.* **231**, 41–52.
- Kozasa T., Hasegawa H. and Nomoto K. (1991) Formation of dust grains in the ejecta of SN 1987A. II. *Astron. Astrophys.* **249**, 474–482.
- Lada C. J. and Lada E. A. (2003) Embedded clusters in molecular clouds. *Ann. Rev. Astron. Astrophys.* **41**, 57–115.
- Lee T., Papanastassiou D. A. and Wasserburg G. J. (1976) Demonstration of ^{26}Mg excess in Allende and evidence for ^{26}Al . *Geophys. Res. Lett.* **3**, 109–112.
- Lee T., Shu F. H., Shang H., Glassgold A. E. and Rehm K. E. (1998) Protostellar cosmic rays and extinct radioactivities in meteorites. *Astrophys. J.* **506**, 898–912.
- Limongi M., Straniero O. and Chieffi A. (2000) Massive stars in the range 13–25 M_{\odot} : evolution and nucleosynthesis. II. The solar metallicity models. *Astrophys. J. Suppl. Ser.* **129**, 625–664.
- Liu M.-C., McKeegan K. D., Davis A. M. and Ireland T.-R. (2007) Beryllium-10 in CM hibonites: implications for an irradiation origin. *Chronol. Meteorit. Early Sol. Syst.* **102**, 103.
- Lodders K. (2003) Solar system abundances and condensation temperatures of the elements. *Astrophys. J.* **591**, 1220–1247.
- Lynden-Bell D. and Pringle J. E. (1974) The evolution of viscous discs and the origin of the nebular variables. *Mon. Not. R. Astron. Soc.* **168**, 603–637.
- MacPherson G. J. (2003) Calcium–aluminum–rich inclusions in chondritic meteorites. In *Treatise of Geochemistry* (eds. H. D. Holland and K. K. Turekian) vol. 1, *Meteorites, Comets and Planets* (ed. A. M. Davis). Elsevier-Pergamon, Oxford. pp. 201–246.
- MacPherson G. J., Davis A. M. and Zinner E. K. (1995) The distribution of aluminum-26 in the early Solar System – a reappraisal. *Meteoritics* **30**, 365.
- MacPherson G. J., Huss G. R. and Davis A. M. (2003) Extinct Be-10 in type A calcium–aluminum–rich inclusions from CV chondrites. *Geochim. Cosmochim. Acta* **67**, 3165–3179.
- Marhas K. K., Goswami J. N. and Davis A. M. (2002) Short-lived nuclides in hibonite grains from Murchison: Evidence for solar system evolution. *Science* **298**, 2182–2185.
- Mathis J. S., Rumpl W. and Nordsieck K. H. (1977) The size distribution of interstellar grains. *Astrophys. J.* **217**, 425–433.
- McCaughrean M. J. and O’dell C. R. (1996) Direct imaging of circumstellar disks in the Orion nebula. *Astron. J.* **358**, 1977–1987.
- McKeegan K. D., Chaussidon M. and Robert F. (2000) Incorporation of short-lived Be-10 in a calcium-aluminum-rich inclusion from the Allende meteorite. *Science* **289**, 1334–1337.
- Meyer B. S. (2005) Synthesis of short-lived radioactivities in a massive star. In *Chondrites and the Protoplanetary Disk* (eds. A. N. Krot, E. R. D. Scott and B. Reipurth). Astronomical Society of the Pacific, San Francisco, pp. 515–526.
- Meyer B. S. and Clayton D. D. (2000) Short-lived radioactivities and the birth of the sun. *Space Sci. Rev.* **92**, 133–152.
- Meyer B. S., Weaver T. A. and Woosley S. E. (1995) Isotope source table for a 25 M_{\odot} supernova. *Meteoritics* **30**, 325.
- Meyer B. S., Nichols R. H., Podosek F. A. and Jennings C. L. (1999) Subtleties in computing anomalies from late nucleosynthetic additions to the proto-solar nebula. *Lunar Planet. Inst. Conf. Abstr.* **30**, 1904.
- Miki J., Takigawa A., Tachibana S. and Huss G. R. (2007) The birth environment of the solar system inferred from a “mixing-fallback” supernova model. *Lunar Planet. Sci.* **XXXVIII**, #1493.
- Morgan H. L., Dunne L., Eales S. A., Ivison R. J. and Edmunds M. G. (2003) Cold dust in Kepler’s supernova remnant. *Astron. J.* **597**, L33–L36.
- Mostefaoui S., Lugmair G. W. and Hoppe P. (2005) Fe-60: A heat source for planetary differentiation from a nearby supernova explosion. *Astrophys. J.* **625**, 271–277.
- Nichols, Jr., R. H., Podosek F. A., MeyerJennings B. S. and Jennings C. L. (1999a) Collateral consequences of the inhomogeneous distribution of short-lived radionuclides in the solar nebula. *Lunar Planet. Inst. Conf. Abstr.* **30**, 1790.
- Nichols, Jr., R. H., Podosek F. A., Meyer B. S. and Jennings C. L. (1999b) Collateral consequences of the inhomogeneous distribution of short-lived radionuclides in the solar nebula. *Meteorit. Planet. Sci.* **34**, 869–884.

- Nittmann J., Falle S. A. E. G. and Gaskell P. H. (1982) The dynamical destruction of shocked gas clouds. *Mon. Not. R. Astron. Soc.* **201**, 833–847.
- Oliveira J. M., Jeffries R. D., van Loon J. T., Littlefair S. P. and Naylor T. (2005) Circumstellar discs around solar mass stars in NGC 6611. *Mon. Not. R. Astron. Soc.* **180**, 21–24.
- Ouellette N., Desch S. J., Hester J. J. and Leshin L. A. (2005) A nearby supernova injected short-lived radionuclides into our protoplanetary disk. In *Chondrites and the Protoplanetary Disk* (eds. A. N. Krot, E. R. D. Scott and B. Reipurth). Astronomical Society of the Pacific, San Francisco, pp. 527–538.
- Ouellette N., Desch S. J. and Hester J. J. (2007a) Interaction of supernova ejecta with nearby protoplanetary disks. *Astrophys. J.* **662**, 1268–1281.
- Ouellette N., Desch S. J. and Hester J. J. (2007b) Injection of supernova dust grains into protoplanetary disks. *Meteorit. Planet. Sci. Suppl.* **42**, 5036.
- Quitté G. and Markowski, A. (2007) Intercalibration of short-lived and long-lived chronometers based on angrites and CB, CR chondrites. *Workshop on Chronology of Meteorites*. #4063 (abstr.).
- Quitté G., Halliday A. N., Meyer B. S., Markowski A., Lattkoczy C. and Guenter D. (2007) Correlated iron 60, nickel 62, and zirconium 96 in refractory inclusions and the origin of the solar system. *Astrophys. J.* **655**, 678–684.
- Rauscher T., Heger A., Hoffman R. D. and Woosley S. E. (2002) Nucleosynthesis in massive stars with improved nuclear and stellar physics. *Astrophys. J.* **576**, 323–348.
- Regelsohn M., Elliott T. and Coath C. D. (2008) Nickel isotope heterogeneity in the early Solar System. *Earth Planet. Sci. Lett.* **272**, 330–338.
- Reynolds J. H. (1960) I-Xe Dating of Meteorites. *J. Geophys. Res.* **65**, 3843–3846.
- Rho J., Kozasa T., Reach W. T., Smith J. D., Rudnick L., DeLaney T., Ennis J. A., Gomez H. and Tappe A. (2008) Freshly formed dust in the Cassiopeia A supernova remnant as revealed by the Spitzer space telescope. *Astrophys. J.* **673**, 271–282.
- Sahijpal S. and Goswami J. N. (1998) Refractory phases in primitive meteorites devoid of ^{26}Al and ^{41}Ca : representative samples of first Solar System solids? *Astrophys. J.* **509**, L137–L140.
- Sahijpal S., Goswami J. N., Davis A. M., Grossman L. and Lewis R. S. (1998) A stellar origin for the short-lived nuclides in the early Solar System. *Nature* **391**, 559–561.
- Shu F. H., Shang H. and Lee T. (1996) Toward an astrophysical theory of chondrites. *Science* **271**, 1545–1552.
- Shu F. H., Shang H., Lee T. and Glassgold A. E. (1997) The origin of chondrites and extinct radioactivities in the solar system. *Bull. Am. Astron. Soc.* **29**, 845.
- Shu F. H., Shang H., Gounelle M., Glassgold A. E. and Lee T. (2001) The origin of chondrules and refractory inclusions in chondritic meteorites. *Astrophys. J.* **548**, 1029–1050.
- Shukolyukov A. and Lugmair G. W. (1993a) Live iron-60 in the early solar system. *Science* **259**, 1138–1142.
- Shukolyukov A. and Lugmair G. W. (1993b) Fe-60 in eucrites. *Earth Planet. Sci. Lett.* **119**, 159–166.
- Smith N., Bally J. and Morse J. A. (2003) Numerous protoplanetary candidates in the harsh environment of the Carina nebula. *Astrophys. J.* **587**, 105–108.
- Srinivasan G., Sahijpal S., Ulyanov A. A. and Goswami J. N. (1996) Ion microprobe studies of Efremovka CAIs.2. Potassium isotope composition and Ca-41 in the early solar system. *Geochim. Cosmochim. Acta* **60**, 1823–1835.
- Srinivasan G., Goswami J. N. and Bhandari N. (1999) Al-26 in eucrite Piplia Kalan: plausible heat source and formation chronology. *Science* **284**, 1348–1350.
- Sugerman B. E. K. et al. (2006) Massive-star supernovae as major dust factories. *Science* **313**, 196–200.
- Tachibana S. and Huss G. R. (2003) The initial abundance of Fe-60 in the solar system. *Astrophys. J.* **639**, L87–L90.
- Tachibana S., Huss G. R., Kita N. T., Shimoda G. and Morishita Y. (2006) Fe-60 in chondrites: debris from a nearby supernova in the early solar system? *Astrophys. J.* **588**, L41–L44.
- Tachibana S., Takigawa A., Miki J. and Yoshida T. (2007) A mixing-fallback supernova as a possible source of short-lived radionuclides in the early solar system. *Workshop on the Chronology of Meteorites and the Early Solar System*. #4079 (abstr.).
- Takigawa A., Miki J., Tachibana S. and Huss G. R. (2007) Contribution of a “mixing-fallback” supernova to short-lived radionuclides in the solar system. *Lunar Planet Sci.* **XXXVIII**, #1720.
- Thrane K., Bizzarro M. and Baker J. A. (2006) Extremely brief formation interval for refractory inclusions and uniform distribution of ^{26}Al in the early solar system. *Astrophys. J.* **646**, L159–L162.
- Thrane K., Nagashima K., Krot A. N. and Bizzarro M. (2008) Discovery of a new FUN CAI from a CV carbonaceous chondrite: Evidence for multistage thermal processing in the protoplanetary disk. *Astrophys. J.* **680**, L141–L144.
- Timmes F. X., Woosley S. E. and Weaver T. A. (1995) Galactic chemical evolution: hydrogen through zinc. *Astrophys. J. Suppl. Ser.* **98**, 617–658.
- Vanhala H. A. T. and Boss A. P. (2000) Injection of radioactivities into the presolar cloud: convergence testing. *Astrophys. J.* **538**, 911–921.
- Vanhala H. A. T. and Boss A. P. (2002) Injection of radioactivities into the forming Solar System. *Astrophys. J.* **575**, 1144–1150.
- Vanhala H. A. T. and Cameron A. G. W. (1998) Numerical simulations of triggered star formation. I. Collapse of dense molecular cloud cores. *Astrophys. J.* **508**, 291–307.
- Wadhwa M., Amelin Y., Davis A. M., Lugmair G. W., Meyer B., Gounelle M. and Desch S. J. (2007) From dust to planetesimals: implications for the solar protoplanetary disk from short-lived radionuclides. In *Protostars and Planets V* (eds. B. Reipurth, D. Jewitt and K. Keil). University of Arizona Press, Tucson, pp. 835–848.
- Wasserburg G. J., Busso M., Gallino R. and Raiteri C. M. (1994) Asymptotic giant branch stars as a source of short-lived radioactive nuclei in the solar nebula. *Astrophys. J.* **424**, 412–428.
- Wasserburg G. J., Busso M. and Gallino R. (1996) Abundances of actinides and short-lived nonactinides in the interstellar medium: Diverse supernova sources for the r-processes. *Astrophys. J.* **466**, L109–L113.
- Wasserburg G. J., Busso M., Gallino R. and Nollette K. M. (2006) Short-lived nuclei in the early solar system: possible AGB sources. *Nucl. Phys. A* **777**, 5–69.
- Weidenschilling S. J. (1977) Aerodynamics of solid bodies in the solar nebula. *Mon. Not. R. Astron. Soc.* **180**, 57–70.
- Williams J. P. and Gaidos E. (2007) On the likelihood of supernova enrichment of protoplanetary disks. *Astrophys. J.* **663**, L33–L36.
- Wooden D. H., Rank D. M., Bregman J. D., Witteborn F. C., Tielens A. G. G. M., Cohen M., Pinto P. A. and Axelrod T. S. (1993) Airborne spectrophotometry of SN 1987A from 1.7 to 12.6 microns – time history of the dust continuum and line emission. *Astron. J. Suppl. Ser.* **88**, 477–507.
- Young E. D., Simon J. I., Galy A., Russell S. S., Tonui E. and Lovera O. (2005) Supra-canonical Al-26/Al-27 and the residence time of CAIs in the solar protoplanetary disk. *Science* **308**, 223–227.